ELSEVIER

Contents lists available at ScienceDirect

## Algal Research

journal homepage: www.elsevier.com/locate/algal





## Design of a E-caprolactam-based ionic liquids for the extraction of lipids from starved *Parachlorella kessleri* microalgae for sustainable aviation fuels (SAF)

Denisse Rivas-Navia, Jacky CheikhWafa, Alba Zurita, Esther Torrens, Christophe Bengoa

Universitat Rovira i Virgili, Departament d'Enginyeria Química, Avinguda dels Països Catalans 26, 43007, Tarragona, Spain

#### ARTICLE INFO

#### Keywords:

Brønsted ε-caprolactam based ionic liquids Green extraction techniques Sustainable aviation fuels Microalgal biorefinery Lipid recovery optimization COSMO-RS

#### ABSTRACT

Sustainable and efficient microalgae lipid extraction methods for the advancement of third-generation biofuels is crucial to propel the decarbonization of the transport sector. Within this context, COCPIT European project is working on the decarbonization of the aviation and marine transports through the exploration of different biofuel production routes from microalgae.

The present study aimed to design, synthesize, and validate four bio-based ionic liquids based on  $\epsilon$ -caprolactam, combined with various organic anions (lactate, acetate, formate, and citrate), to extract lipids from starved *Parachlorella kessleri* for the production of sustainable aviation fuels (SAF). The Brønsted-type ionic liquids were synthetised using acid-base neutralization reactions.

The lipid extraction efficiency of each ionic liquid was first evaluated, with  $\epsilon$ -caprolactam-lactate (CPL-LAC) leading to the highest recovery, 89.80 %. The ionic liquids performance was validated with COSMO-RS calculations to have a more solid rationale for ionic liquid selection. Although caprolactam-lactate ionic liquid ranked third in the COSMO-RS affinity predictions, it was selected for response surface design optimization due to its experimental performance and the lack of significant differences between the ionic liquids.

Caprolactam-lactate ionic liquid, in turn, exhibited outstanding physicochemical properties, such as high thermal stability (TGA: 198.60 °C), low melting point (DSC: -3.75 °C), and a strong ability to facilitate molecular interaction, as shown in NMR and FTIR spectroscopy. The lipid extraction process with caprolactam-lactate ionic liquid was optimized through surface response analysis, which required a total of 31 experiments. The optimized conditions (42 °C, biomass:ionic liquid ratio 1:11, 8 h of stirring, 19 min of sonication) led to extraction efficiencies within 89.60 % and 91.80 %. The recovered lipids were esterified and analysed through gas chromatography-FID in terms of fatty acid methyl esters (FAMEs) composition. The most predominant FAMEs were palmitic (C16:0), stearic (C18:0), and oleic (C18:1 cis + tras) acids, suggesting the suitability of the obtained extract in biofuel applications.

## 1. Introduction

One of the greatest challenges of the aviation industry is the reduction of its carbon emissions to ensure its environmental sustainability in the long run [1,2]. As a result, the development of sustainable aviation fuels (SAF) has become one of the cornerstones to overcome such challenges. The use of biomass as a fuel feedstock propels the production of clean [3] and renewable energy and aligns with the Sustainable Development Goals (SDGs) [4,5].

From the many biomass sources available for such end, microalgae have gained considerable interest due to their high productivity, rapid growth rates [6], and their ability to accumulate valuable metabolites such as carbohydrates, proteins, and lipids [7]. These microalgae-based biofuels, also known as third-generation biofuels, have become increasingly relevant in the global context of decarbonization and energy transition, where fossil fuels are being gradually replaced by more sustainable alternatives [8].

One of the most attractive features of microalgae for SAF production is their lipogenic potential, they can rapidly accumulate lipids containing essential fatty acids crucial for high-value components such as eicosapentaenoic acid (EPA, 20:5n-3) and docosahexaenoic acid (DHA, 22:6n-3) [9]. This trait has been acknowledged since the mid - 20th

E-mail address: christophe.bengoa@urv.cat (C. Bengoa).

<sup>\*</sup> Corresponding author.

century and consists in cells' accumulation of neutral lipids such as triacylglycerols (TAGs) when exposed to nutrient stress conditions [10]. Nitrogen deficiency is one of these possible stress mechanisms in microalgae cultures, which leads to the transformation of their polyunsaturated fatty acid (PUFA)-rich membrane lipids into storage lipids enriched in saturated fatty acids (SFA) [11]. In this context, biofuels based on fatty acid methyl esters (FAMEs) have attracted growing attention [12].

Parachlorella kessleri is a freshwater microalga that has a strong potential for biofuel production. It can be used for bioethanol production from its starch content, and also for biodiesel or SAF production from its lipids. The latter is due to its increase in lipid accumulation when cultured following nutrient limitation strategies, such as cultivation in diluted mineral media [10,13].

Still, it must be noted that conventional lipid extraction methods from microalgae rely on organic solvent mixtures, as is the case of the Folch [14], Bligh and Dyer [15] and Hara and Radin [16] methods. While effective, these extraction schemes pose environmental concerns and present challenges for their large-scale industrial application. To tackle this issue, ionic liquids (ILs) have emerged as a greener alternative solvent. ILs are pure compounds formed by a cation and an anion (i.e., salts) and are mostly found in liquid state at room temperature [17]. They are characterized by their excellent thermodynamic stability and high solvation capacity [18,19] and, are increasingly recognized as ecofriendly solvents and novel catalytic media [20]. Their "designer solvent" properties, due to the tunability of both the cation and anion, make them particularly attractive for targeted applications [21,22].

From the many ILs known to date, bio-based ILs are a group of ILs derived from renewable sources, such as  $\varepsilon$ -caprolactam. Bio-based ILs show lower toxicity [23] and higher recyclability than some common ILs, while having selective affinity for neutral lipids [24,25]. Some studies have proved that ILs such as caprolactam-formate and caprolactam-acetate can outperform traditional solvent-based methods [26], achieving lipid recoveries greater than 55 % in species such as Chlorella and Chlorococcum [24,27-29]. Currently, the literature also highlights limitations in the use of ionic liquids, such as the high cost associated with the use of large volumes and the lack of studies on recyclability and environmental toxicity, this has led to the need to explore new families of ILs that are more economical and sustainable [9]. Therefore, the use of caprolactam-based ionic liquids is an attractive alternative because  $\varepsilon$ -caprolactam is a low-cost and widely available monomer whose structure allows the design of ILs with adjustable properties that can be biodegradable [29].

The present study is framed within the COCPIT project (Scalable solutions optimisation and decision tool creation for low impact SAF production chain from lipid-rich microalgae strain), funded by the European Union's Horizon Europe Research and Innovation Programme (Grant Agreement No. 101122101). COCPIT aims to demonstrate the technical, economic, and environmental feasibility of a novel, sustainable biorefinery model for SAF production through the cultivation of microalgae and their subsequent biochemical conversion into biofuels through two alternative pathways. In one of these pathways, lipids extracted from starved *Parachlorella kessleri* are subjected to hydrodeoxygenation reactions to yield medium and long-chain hydrocarbons compatible with ASTM D7566 standards for aviation fuel (Abrantes et al. 2021).

The efficiency of this conversion pathway largely depends on the ability to selectively extract target lipids while minimizing the use of toxic solvents, enhancing the sustainability of the process. Despite the existence of previous works where ionic liquids based on caprolactam (caprolactam-formate/acetate or butyrolactam-hexanoate) are used for the lysis and extraction of lipids from microalgae [27], in these studies no molecular modeling support or statistical optimization of the process has been carried out, therefore, this work aims to optimize and validate lipid extraction from *Parachlorella kessleri* cultivated under stress conditions using bio-based ILs composed of  $\varepsilon$ -caprolactam as the cation and

various organic acid-derived anions (lactate, acetate, formate, and citrate).

The proposed experimental strategy combines preliminary experimental screenings of ILs with the use of COSMO-RS to validate experimental observations. COSMO-RS (Conductor-like Screening Model for Real Solvents) is a molecular simulation software that allows the prediction of IL-solute affinities, facilitating the selection of the most suitable solvents for a targeted purpose and that has been used in the extraction of microalgal products [30–32]. Both the experimental screening and theoretical calculations allowed the selection of the most suitable IL, whose extraction ability was optimized through Response Surface Methodology (RSM). This methodology not only provides a rational approach to select alternative solvents like bio-based ILs, but also paves the way for the optimization of processes within microalgae biorefinery development.

## 2. Materials and methods

#### 2.1. Materials

For the Lowry method: sodium hydroxide (purity >97 %), concentrated sulfuric acid (purity 97 %), anhydrous sodium carbonate (Na<sub>2</sub>CO<sub>3</sub>, ACS reagent), copper (II) sulfate pentahydrate (CuSO<sub>4</sub>·5H<sub>2</sub>O), potassium sodium tartrate tetrahydrate (purity 99 %), Folin-Ciocalteu's phenol reagent and bovine serum albumin (BSA) were purchased from Sigma Aldrich. For the Dubois method: glucose monohydrate was obtained from Sigma-Aldrich. A phenol solution at 82 % (w/v) was freshly prepared using crystalline phenol supplied by PanReac AppliChem. For the Bligh and Dyer method: chloroform and hexane were both acquired from Sigma-Aldrich. For the synthesis of ILs:  $\varepsilon$ -Caprolactam (purity  $\geq$ 99 %) was supplied by Sigma-Aldrich, lactic acid (purity ≥90 %) and acetic acid (purity ≥99.8 %) were purchased from Fluka, formic acid (purity  $\geq$ 98 %) of J.T. Baker<sup>TM</sup>, citric acid (purity  $\geq$ 99.5 %) and absolute ethanol of analytical grade was provided by Scharlau S.L. For the esterification process of fatty acid methyl esters (FAMEs): hexane, sulfuric acid (purity >97 %), methanol (purity >99 %), sodium chloride and sodium bicarbonate were all supplied by Sigma-Aldrich. Distilled water was used in all experiments.

## 2.2. Microalgae

## 2.2.1. Growth, collection and management

Parachlorella kessleri UTEX 2229 (Austin, Texas, USA) was produced in the AlgoSolis facility (Nantes University, CNRS, UAR 3722, Saint-Nazaire, France) using a modified Bold Basal medium consisting of: Na<sub>2</sub>EDTA·2H<sub>2</sub>O (0.13 mM), MgSO<sub>4</sub>·7H<sub>2</sub>O (0.91 mM), K<sub>2</sub>HPO<sub>4</sub> (0.86 mM), KH<sub>2</sub>PO<sub>4</sub> (0.90 mM), CaCl<sub>2</sub>·2H<sub>2</sub>O (0.04 mM), FeSO<sub>4</sub>·7H<sub>2</sub>O (0.050 mM), ZnSO<sub>4</sub>·7H<sub>2</sub>O (7.72  $\times$  10<sup>-4</sup> mM), CuSO<sub>4</sub> (4.95  $\times$  10<sup>-4</sup> mM), MnCl<sub>2</sub>·4H<sub>2</sub>O (9.15  $\times$  10<sup>-3</sup> mM), H<sub>3</sub>BO<sub>3</sub> (0.05 mM), CO(NO<sub>3</sub>)<sub>2</sub>·6H<sub>2</sub>O  $(1.51 \times 10^{-4} \text{ mM})$ , Na<sub>2</sub>MoO<sub>4</sub>  $(1.06 \times 10^{-3} \text{ mM})$ , NaHCO<sub>3</sub> (5.00 mM). Since culture stress was induced via nitrogen deprivation, no NaNO<sub>3</sub> was added to the culture medium. Cultivation was conducted in a 180 L flatpanel airlift photobioreactor (HECtor PBR) operated indoors and in batch mode. The reactor's pH was kept at 8, and its stability was ensured with a pH self-regulating system by pure CO2 injection. Light conditions were manually adjusted according to the culture evolution by regulating the artificial light intensity of its LED panels (The LEDs panels had white light, and their intensity was adjusted based on the culture evolution). Biomass harvesting was conducted using a continuous centrifugal system (DRA320VX Rousselet Robatel, France) operating at 6000 rpm to obtain a microalgal sludge of approximately 250 g/L. This wet biomass was stored in a freezer at  $-20\,^{\circ}\text{C}$  and then transported to Spain at such temperature conditions.

## 2.2.2. Microalgae characterization

A full characterization of Parachlorella kessleri samples was

performed in triplicate. Moisture, total solids (TS), volatile solids (VS) and ash content were analysed following the standard method 2540B [33]. The quantification of carbohydrates was carried out following exactly the methodology described by Dubois et al. [34]. Protein quantification was conducted using the Lowry method [35]. Lipid content was determined using the Bligh and Dyer method [15].

#### 2.3. $\varepsilon$ -caprolactam-based ionic liquids

## 2.3.1. Ionic liquid synthesis

Four novel Brønsted acidic ionic liquids (ILs) based on lactams were synthetised following a one-step synthesis, that is, a simple atom-economical neutralization reaction. The synthesis involved the mixture of  $\epsilon$ -caprolactam with each of the four selected acids (acetic, citric, formic and lactic). Fig. 1 presents the synthesis scheme of  $\epsilon$ -caprolactam-based ionic liquids.

 $\epsilon$ -caprolactam (11.32 g or 0.10 mol) and H<sub>2</sub>O (10 mL) were mixed in a round flask until a clear solution was obtained. Then, the desired acid (acetic, citric, formic or lactic) (0.10 mol) was added dropwise to the flask, which was immersed in an ice bath. The sample was left under constant magnetic stirring for 12 h at 50 °C. H<sub>2</sub>O was subsequently evaporated in the rotary evaporator at 40 mbar for 30 min. The resulting mixture was washed with absolute ethanol to remove any unreacted products before filtration. The organic solvent (ethanol) was finally removed via evaporation at 90 mbar for 30 min.

## 2.3.2. Ionic liquids characterization

 $\epsilon$ -caprolactam-acetate (CPL-Acet),  $\epsilon$ -caprolactam-citrate (CPL-Cit),  $\epsilon$ -caprolactam-formate (CPL-For) and  $\epsilon$ -caprolactam-lactate (CPL-Lac) were subjected to different analyses, such as nuclear magnetic resonance (NMR), thermogravimetric analysis (TGA), differential scanning calorimetry (DSC), and Fourier-transform infrared spectroscopy (FTIR).

2.3.2.1. Nuclear magnetic resonance (NMR). A sample of approximately 50 mg was diluted in deuterated water and placed in 5 mm diameter NMR tubes. <sup>1</sup>H NRM and <sup>13</sup>C NRM were completed in Bruker Avance III NMR spectrometer in the scientific and technical resources service of the Universitat Rovira i Virgili.

2.3.2.2. Thermogravimetric analysis (TGA). To determine the thermal stability of the IL, a TGA analysis was performed under a nitrogen atmosphere within a temperature range from 25 to 400 °C with a heating rate of 10 °C/min. Approximately 50 mg of sample were placed in aluminium crucibles and analysed by a Mettler Toledo TGA/SDTA851 equipment with a MT1 type balance. The analysis was done at the Institut Català d'Investigació Química (Catalan Institute of Chemical Research, ICIQ).

2.3.2.3. Differential scanning calorimetry (DSC). To determine the melting point of IL, DSC analysis was performed using a Mettler Toledo DSC822 equipment with a 56-point Au-AuPd thermopile FRS5 sensor. The analyses were conducted over a temperature range from -80 to 90 °C and a scan rate of 5 °C/min, under a nitrogen flow of 50 mL/min. 6 cycles (3 for heating and 3 for cooling) were performed to understand the thermal behaviour of the IL and its suitability for specific

applications. The samples were analysed at the Institut Català d'Investigació Química (Catalan Institute of Chemical Research, ICIQ).

2.3.2.4. Fourier-transform infrared spectroscopy FTIR. FTIR of the ionic liquids was done using the spectrophotometer IR Jasco FT/IR-6700 of the scientific and technical resources service of the Universitat Rovira i Virgili. The spectra were observed between 4000 a 500 cm $^{-1}$  with a resolution of  $0.98~{\rm cm}^{-1}$ .

2.3.2.5. Density and pH. The density of the samples was gravimetrically determined at 20  $^{\circ}$ C with a calibrated pycnometer [36]. The pH was measured using a potentiometer (Crison GLP 21) previously calibrated with standard buffer solutions.

# 2.4. Lipid extraction from starved Parachlorella kessleri with $\varepsilon$ -caprolactam ionic liquids

### 2.4.1. General procedure

The general lipid extraction process employed both in the IL screening and the extraction optimization is described in Fig. 2. Starved *Parachlorella kessleri*, as received, was pre-treated for cell disruption using Hielscher Ultrasonics GMBH ultrasound, equipped with a 7.00 mm sonotrode, operating at 0.50 cycles and with an amplitude of 80 %.

Then, 4.00 g of wet microalgae, containing 1.00 g of total solids, was mixed with the IL at a given ratio. The mixture was kept under constant magnetic stirring at 600 rpm at a given time and temperature.

After extraction completion, the mixture was allowed to cool down to room temperature. 10 mL of methanol were subsequently added to precipitate the solids. This step was followed by the addition of 10 mL of hexane. The samples were vortexed for 30 s to ensure their homogenization before undergoing centrifugation at 4000 rpm for 5 min (Thermo Scientific<sup>TM</sup> Sorvall<sup>TM</sup> ST 16R, rotor F15-6 x 100y).

After this, three phases were obtained: a solid phase (precipitate), an intermediate phase consisting of the ionic liquid, methanol and water, and an upper phase containing the hexane and lipids.

The upper phase was removed using a Pasteur pipette. The washing process with hexane was repeated several times until obtaining a clear and transparent upper phase. The lipids extracted in hexane were washed with 20 mL of deionized water to remove possible impurities. The mixture was stirred, and phase separation was allowed to occur through a liquid-liquid extraction funnel. The lower part, containing water and impurities, was removed. This washing procedure was repeated three times to ensure the complete removal of impurities. The recovered lipids and hexane were transferred to a pre-weighed round-bottom flask to evaporate hexane in a rotary evaporator. The rotary evaporator operated at 60 °C and 360 mbar vacuum, allowing lipid recovery on the flask after hexane evaporation. The percentage of lipids recovered was gravimetrically calculated with the following equation (Eq. (1)):

lipids yield% = 
$$\frac{W_{lipids}(g)}{\left(W_{TS}(g) x \frac{\% Lipids_{sample}}{100} *100\right)} *100$$
 (1)

Where lipids are the weight of lipids after evaporation of hexane and

Fig. 1. Synthesis of ionic liquid based on ε-caprolactam and lactic acid. Synthesis of ionic liquids based on citric, formic and acetic acids is identical.

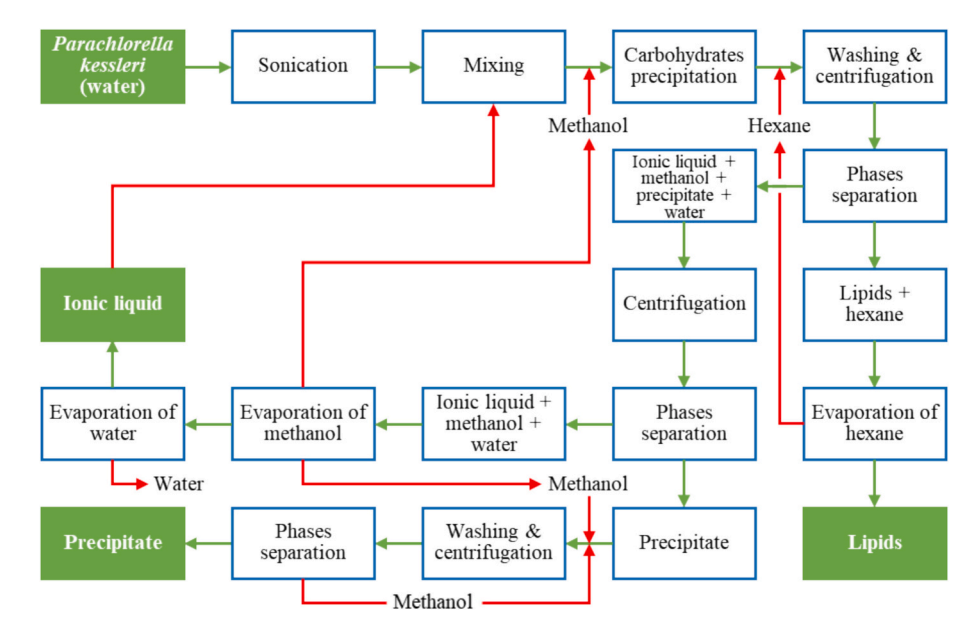


Fig. 2. Scheme of lipids extraction process from starved Parachlorella kessleri by ε-2caprolactam ionic liquids.

 $W_{TS}$  is the initial weight of total solids of the 1.00 g sample, % Lipids<sub>sample</sub> is the total percentage of lipids contained in the microalgae sample.

2.4.2. Lipid extraction screening using different  $\varepsilon$ -caprolactam-based ionic liquids

2.4.2.1. Experimental screening. The four caprolactam-based ILs, CPL-Acet, CPL-Git, CPL-For and CPL-Lac were first evaluated in terms of lipid recovery. Each extraction was performed in triplicate. Table 1 presents the extraction conditions.

2.4.2.2. Computational study of the interaction of  $\epsilon$ -caprolactam ionic liquid with lipids. COSMO-RS (COnductor-like Screening MOdel for Realistic Solvents) [37] was used to evaluate the interaction of the three major lipids of Parachlorella kessleri, oleic, linoleic and  $\alpha$ -linolenic acid, with the four different ionic liquids evaluated in this work at the screening temperature, 80 °C. Such interactions were assessed in terms of logarithmic infinite dilution activity coefficients (In  $\gamma^\infty$ ) and  $\sigma$  profiles.

The COSMO-files of the cation (caprolactam), the anions (acetate, citrate, formate and lactate) and the three lipids were obtained via geometry optimization at GGA: BP86 density functional level and TZP (triple- $\zeta$  polarization) basis set with the ADF (Amsterdam Density Functional) package [38]. These files were then used to calculate the ln  $\gamma^{\infty}$  and  $\sigma$  profiles with COSMO-RS. Both ADF and COSMO-RS calculations were conducted using the 2024.1 version of the Amsterdam Modeling Suite [39] by SCM software (Software for Chemistry and Materials BV, Amsterdam, The Netherlands) (AMS 2024.1 COSMO-RS, SCM).

To calculate the  $\ln \gamma^{\infty}$  of each lipid in each ionic liquid at 50 °C, the

Table 1 Extraction condition of lipid's extraction process of microalgae Parachlorella kessleri using different  $\epsilon$ -caprolactam-based ionic liquids.

Experimental condition	Value
Ratio	1:10 g <sub>Microalgae</sub> /g <sub>Ionic Liquid</sub>
Temperature Speed of stirring	500 rpm
Time of stirring	5 h
Time of sonication	20 min

ionic liquids were treated as individual sets of cations and anions mixed in a proportion that would ensure ionic liquid neutrality [40]. The calculation of these coefficients employed the COSMO-RS reparameterization for ionic liquids, ADF Lei2018, as it is considered more accurate for systems involving ILs [41].

2.4.3. Optimization of the extraction conditions with design of experiments

The lipid extraction efficiency of the best-performing IL was optimized using design of experiments (DOE) with Minitab®. The selected approach was response surface methodology (RSM) following a fourfactor Central Composite Design (CCD). CCD allowed the study of the impact of four independent factors, temperature, stirring time, ratio (biomass: ionic liquid) and the duration of sonication as pre-treatment, in the recovery of microalgae lipids.

Each of the variables was coded as 2 (maximum), 1 (high), 0 (central), -1 (low), and -2 (minimum). Table 2 shows the codification of the experimental values for each of the variables used in the experimental design. The ranges selected for each variable were defined with the purpose of achieving an efficient and economically viable extraction process, also allowing to evaluate the individual and combined influence of the operating conditions on the lipid yield. For temperature, a range from 20 °C to 100 °C was established, with the lower limit being representative of ambient temperature and the upper limit based on previous literature reporting optimal extraction efficiencies in that range [42]. The intermediate temperatures (40 °C, 60 °C and 80 °C) were computed by the software and allowed the study of the thermal gradients with potential effect on process efficiency.

Regarding the biomass:ionic liquid ratio, extreme values, from 1:1 to 1:13, were explored with the aim of optimizing the ratio of reagents used. The computed intermediate levels (1:4, 1:7, 1:10) were defined by the software, but the latter of these three calculated values has been reported as optimal in previous studies [42].

 Table 2

 Values and codes used in the experimental design.

Experimental condition	Code						
	-2	-1	0	1	2		
Temperature (°C)	20	40	60	80	100		
Ratio (biomass:ionic liquid)	1:1	1:4	1:7	1:10	1:13		
Time of sonication (min)	0	10	20	30	40		
Time of stirring (min)	0	2	4	6	8		

For the sonication time, a maximum of 40 min was defined to avoid the overheating of the samples and possible biomass degradation, while the minimum was set at 0 min (no sonication), to evaluate whether the application of ultrasounds represented a significant factor in the process.

As for the stirring time, extreme values were also considered (0 h and 8 h), as well as intermediate levels with progressive increments of 2 h (2 h, 4 h, 6 h), in order to evaluate its effectiveness.

## 2.5. Esterification of the extracted lipids

## 2.5.1. Experimental procedure

The conversion of the lipids extracted from microalgae to FAMEs was carried out through acid catalysis esterification using a modified version of Christie's method [43]. Around 50 mg of lipids, 1 mL of hexane and 2 mL of a 1 % sulfuric acid solution dissolved in methanol were mixed together and left in a digester at 50 °C overnight. Then, 5 mL of a solution with 5 % of sodium chloride and 5 mL of hexane were added and mixed in the vortex. Two phases were obtained: the upper phase, containing hexane and FAMEs, was removed with a Pasteur pipette, while the lower phase contained the residue. The same process was repeated another time. The upper phase (containing hexane and the FAMEs) was added 4 mL of a 2 % sodium bicarbonate solution and was mixed in a vortex. Two new phases were obtained: an upper phase with the hexane and pure FAMEs, and a lower phase the impurities. This new upper phase was removed and transferred to a pre-weighed round-bottom flask Hexane was evaporated in the rotary evaporator at 360 mbar for 10 min and FAMEs were obtained.

#### 2.5.2. Characterization of products by GC-FID

The FAMEs produced by transesterification were analysed on an Agilent 6890GC gas chromatograph with a flame ionization detector (FID). Separation was achieved on an HP-INNOWax 30 m  $\times$  0.25 mm  $\times$  0.25 mm column (Agilent part no. 19091 N-133I), with helium as the carrier gas and with a constant injector temperature of 260 °C. The sample injection volume was 2.50 L with a split ratio of 20/1. The FID was maintained at 260 °C throughout the analysis. The oven temperature program started from 150 °C, held this temperature for 1 min, and then increased the temperature at a pace of 2.90 °C/min to 230 °C, which was held for 1 min. A standard 37-component mixture of FAMEs was used for instrument calibration. All calibration curves were linear with a correlation coefficient of 0.99 or better. The results of the gas chromatography runs were used to calculate the amount of saponifiable material in the extracted lipids. The amount of saponifiable lipids is expressed by Eq. (2) (Eq. (2)).

$$Saponifiable~(\%) = \frac{FAMEs~(g)}{Lipids~(g)} \times 100 \tag{2}$$

where FAMEs are the total FAMEs produced after transesterification by the reference method, determined by running GC-FID, and Lipids is the amount of lipids used for transesterification.

## 3. Results

### 3.1. Characterization of Parachlorella kessleri

The results obtained in the characterization of *Parachlorella kessleri* are presented in Table 3. *Parachlorella kessleri* contained 25.66 % of total solids, resulting in 74.34 % of moisture content. In the solid part, it had an important volatile content (93.70 %) and small amount (6.30 %) of ashes. The lipid content was very predominant in *Parachlorella kessleri*, 34.83 %, confirming the impact of stress conditions. Ra et al. conducted a two-stage culture based on light stress conditions and observed a maximum lipid content of 56 % of dry cell weight in *Nannochloropsis oculata* under green light stress for 2 days in the second stage of culture [44]. The relationship between culture conditions and the accumulation

 Table 3

 Characterization of microalgae Parachlorella kessleri.

Ingredient	Weight (g)	Percentage (%)
Microalgae sample	1.00 (w/	_
	$w_{TS}$ )	
Total Solids (TS)		$25.70 \pm 0.33 (w/$
		$w_{Biomass}$ )
Moisture (by difference from TS)		74.30 (w/w <sub>Biomass</sub> )
Ashes		$6.30 \pm 0.42  (\text{w/w}_{\text{TS}})$
Volatile Solids (VS, by difference from ashes)		93.70 (w/w <sub>TS</sub> )
Carbohydrates		$29.80 \pm 0.50 (w/w_{VS})$
Proteins		$24.10 \pm 0.82 \ (\text{w/w}_{\text{VS}})$
Lipids		$34.80 \pm 2.16  (w/w_{VS})$
Total mass balance		$88.70  (w/w_{VS})$

of macromolecules such as starch and lipids in *Chlorella and Parachlorella* has also been extensively studied. It indicates that the type of stress applied influences the predominant metabolic pathway, directing synthesis toward carbohydrate or lipid [45]. Under stress conditions, microalgae such as *Parachlorella kessleri* tend to accumulate lipids in large quantities, making them ideal candidates for integrated biorefinery processes [46]. Lipids extracted from microalgae play an important role in the production of sustainable biofuels as they are mostly composed of saturated and monounsaturated fatty acids, which contribute to the thermal and oxidative stability of the fuel, improving its energy efficiency [45].

These results agree with those presented by Vitova et al. [10], who stated that the effect of light intensity can also enhance carbohydrate production as is the case in *C. vulgaris* where percentages of 46 % were obtained. A variation in light intensity of 700 µmol photons/s  $m^2$  in *Nannochloropsis* sp. resulted in a 47 % higher lipid amount [47] and eight algal strains (*Chlorella viscosa, C. vulgaris, Chlorella sorokiniana, C. emersonii, Parachlorella beijerinckii, P. kessleri* CCALA255, NIES-2159 and NIES-2152) increased starch and lipid productivity under high light intensity (600 µmol photons  $m^{-2}$  s $^{-1}$ ) [48]. Like the effect of light intensity, biomass growth rates as well as lipid and starch accumulation increased to some extent with increasing temperature. In *S. obliquus*, the final lipid reserve content ranged from 18 % to 40 % at temperatures between 20 °C and 27.50 °C. Increasing the temperature to a sublethal value (38 °C) caused an increase in lipid content (up to 34 %) in *N. oculata* and *C. vulgaris* [49].

## 3.2. Ionic liquid characterization

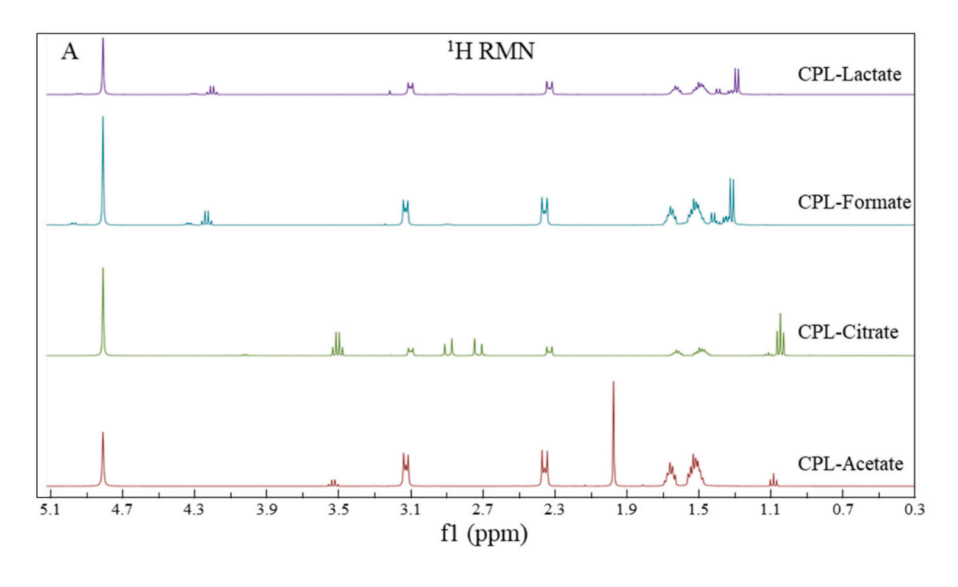
Proton ( $^{1}$ H NMR) and carbon-13 ( $^{13}$ C NMR) nuclear magnetic resonance (NMR) spectroscopy were used to confirm the formation of ionic liquids from  $\epsilon$ - caprolactam (CPL) as the base and different organic acids as proton donors.

Fig. 3A shows the  $^1$ H NMR spectrum, which depicts changes in the position and shape of the peaks compared to the individual spectra of the reactants. Fig. 3B, the  $^{13}$ C NMR spectrum, shows variations in the signals of the carbonyl group and the caprolactam chain. The chemical shifts observed in both spectra reveal the interaction between the amide group of caprolactam and the carboxylic groups of the acids, confirming that the formation of ionic liquids occurred through the specific interaction between  $\epsilon$ -caprolactam and the selected organic acids.

## 3.2.1. ε-caprolactam-lactic acid

 $^{1}{\rm H}$  NMR spectrum (500 MHz;  $\rm D_{2}O)$   $\delta$  (ppm): 1.26 (3H, d, J=7.5 Hz); 1.42 (2H, m, J=7.50 Hz); 1.58 (2H, m, J=7.5 Hz); 2.80 (2H, m, J=7.50 Hz); 3.05 (2H, t, J=7.50 Hz); 4.22 (1H, q, J=7.50 Hz); 4.74 (1H, s) ppm.

<sup>13</sup>C RMN spectrum (62.5 MHz;  $D_2O$ ) δ (ppm): 16.21 (-CH<sub>3</sub>, CPL); 19.34 (-CH<sub>3</sub>, CPL) 22.5 (-CH<sub>2</sub>, CPL); 28.40 (-CH<sub>2</sub>, CPL); 29.80 (-CH<sub>2</sub>, CPL); 35.40 (-CH<sub>2</sub>, CPL); 42.20 (-CH<sub>2</sub>, CPL); 53.40 (-CH, Lac); 66.30 (CH<sub>2</sub>-O, Lac); 178.28 (C=O, Lac); 182.02 (C=O, CPL).



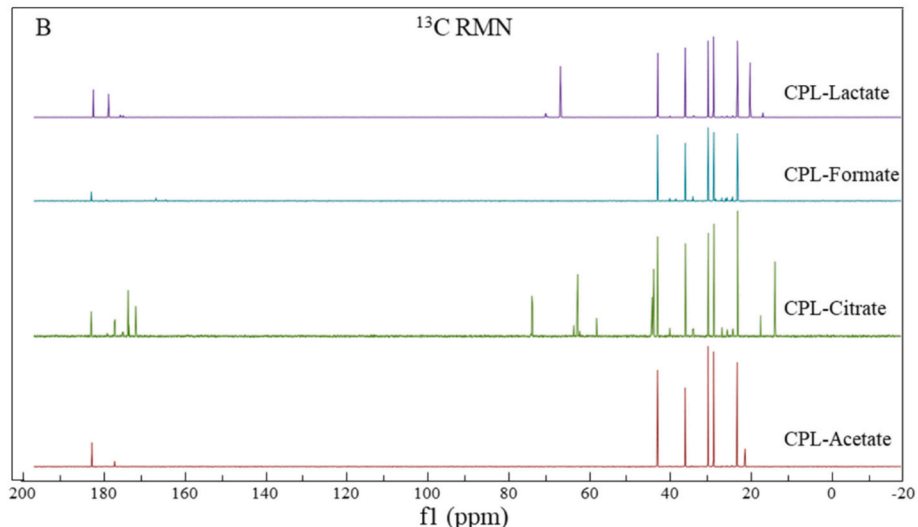


Fig. 3. NMR spectra of the four ε-caprolactam-based ionic liquids: Caprolactam (CPL)-Lactate; Caprolactam-Formate; Caprolactam-Citrate; Caprolactam-Acetate. A:  $^{1}$ H RMN. B:  $^{13}$ C NMR.

## 3.2.2. ε-caprolactam-citric acid

 $^{1}{\rm H}$  NMR spectrum (500 MHz; D<sub>2</sub>O)  $\delta$  (ppm): 1.23 (2H, m, J = 7.5 Hz), 1.53 (2H, m, J = 7.50 Hz), 2.27 (2H, m, J = 7.50 Hz), 2.76 (2H, m, J = 7.50 Hz), 3.06 (2H, m, J = 7.50 Hz), 3.30 (2H, m, J = 7.5 Hz), 3.45 (2H, m, J = 7.50 Hz), 4.74 (1H, s) ppm.

 $^{13}\text{C}$  RMN spectrum (62.50 MHz; D<sub>2</sub>O)  $\delta$  (ppm): 13.90 (-CH<sub>3</sub>); 18.20 (-CH<sub>2</sub>, CPL); 22.50 (-CH<sub>2</sub>, CPL); 28.60 (-CH<sub>2</sub>, CPL); 29.70 (-CH<sub>2</sub>, CPL); 35.40 (-CH<sub>2</sub>, CPL); 41.50 (-CH<sub>2</sub>, CPL); 55.20 (-CH-OH, Cit); 62.50 (CH<sub>2</sub>-OH, Cit); 73.40 (-CH-OH, Cit); 171.30 (C=O, Cit); 172.10 (C=O, Cit); 173.20 (C=O, Cit); 175.60 (C=O, CPL).

## 3.2.3. $\varepsilon$ -caprolactam-formic acid

 $^{1}$ H NMR spectrum (500 MHz; D<sub>2</sub>O)  $\delta$  (ppm): 1.24 (2H, m, J = 7.50 Hz), 1.53 (2H, m, J = 7.50 Hz), 2.34 (2H, m, J = 7.50 Hz), 2.75 (2H, m, J = 7.50 Hz), 3.10 (2H, m, J = 7.50 Hz), 4.20 (1H, q, J = 7.5 Hz), 4.74 (1H, g) ppm.

 $^{13}$ C RMN spectrum (62.50 MHz; D<sub>2</sub>O) δ (ppm): 22.20 (-CH<sub>3</sub>, CPL); 23.00 (-CH<sub>2</sub>, CPL); 25.60 (-CH<sub>2</sub>, CPL); 27.60 (-CH<sub>2</sub>, CPL); 28.90 (-CH<sub>2</sub>, CPL); 30.30 (-CH<sub>2</sub>, CPL); 31.90 (-CH<sub>2</sub>, CPL); 33.90 (-CH<sub>2</sub>, CPL); 42.30 (-CH<sub>2</sub>, CPL); 165.50 (C=O, For); 181.80 (C=O, CPL).

## 3.2.4. $\varepsilon$ -caprolactam-acetic acid

<sup>1</sup>H NMR spectrum (500 MHz; D<sub>2</sub>O)  $\delta$  (ppm): 1.01 (2H, m, J = 7.50

Hz), 1.40 (2H, m, J = 7.50 Hz), 1.61 (2H, m, J = 7.50 Hz), 1.94 (3H, s, J = 7.50 Hz), 2.33 (2H, m, J = 7.50 Hz), 3.11 (2H, m, J = 7.50 Hz), 3.51 (2H, m, J = 7.50 Hz).

 $^{13}\text{C}$  RMN spectrum (62.50 MHz; D<sub>2</sub>O)  $\delta$  (ppm): 20.60 (-CH<sub>3</sub>, CPL); 22.60 (-CH<sub>2</sub>, CPL); 28.40 (-CH<sub>2</sub>, CPL); 29.70 (-CH<sub>2</sub>, CPL); 35.50 (-CH<sub>2</sub>, CPL); 30.30 (-CH<sub>2</sub>, CPL); 31.90 (-CH<sub>2</sub>, CPL); 33.90 (-CH<sub>2</sub>, CPL); 42.30 (-CH<sub>2</sub>, CPL); 176.71 (C=O, Acet); 181.80 (C=O, CPL).

In the FTIR spectra, the appearance of broad O-H/N-H stretching signals in the 3400-3200 cm<sup>-1</sup> region indicated acid-base neutralization and strong hydrogen-bonding interactions between the caprolactam cation and the corresponding anions. These features are consistent with the chemical changes observed in the <sup>1</sup>H and <sup>13</sup>C NMR spectra, confirming the formation of ion pairs and the successful synthesis of the target ILs. The signals emitted by the ionic liquids can be seen in Fig. 6. The absorption at the 3289 cm<sup>-1</sup> peak is attributed to the N—H stretching vibration of  $\epsilon$ -caprolactam, which is consistent with the report by Xu et al. [50], who identified the caprolactam peak at 3207 cm<sup>-1</sup>. The broad band between 3100 and 3500 cm<sup>-1</sup> present in the four ionic liquids represents the superposition of O—H and N—H stretching, indicating the formation of hydrogen bonds between caprolactam and organic acids. The widest and most intense band corresponds to CPL-Lac and CPL-Cit, suggesting greater interaction due to the number of functional groups (-OH and -COOH) in lactic and citric acid. The signals at

2984 and 2931 cm<sup>-1</sup> are commonly related to C-H stretching vibrations in the methyl (CH<sub>3</sub>) and methylene (CH<sub>2</sub>) groups, present in both ε-caprolactam and lactic acid [29]. The peak at 1713 cm<sup>-1</sup> is characteristic of the C=O stretching vibration of the carbonyl groups of caprolactam and carboxylic acids. The signal at 1617 cm<sup>-1</sup> is associated with the C=O stretching vibration of an amide group, characteristic of  $\varepsilon$ -caprolactam [50]. The bands between 1500 and 1650 cm<sup>-1</sup> are N—H and C-N deformations; these bands can be altered by interactions between the amide group of caprolactam and organic acids. The C-H bending vibration, corresponding to the methyl groups, is detected at  $1438 \text{ cm}^{-1}$ . The signals between  $1200 \text{ cm}^{-1}$  and  $1062 \text{ cm}^{-1}$  are attributed to CO stretching vibrations in carboxylic acids and ethers, which is consistent with the structure of lactic acid. Finally, the peak at 821  ${\rm cm}^{-1}$ is associated with out-of-plane bending vibrations of C-H groups, common in the rings of cyclic compounds such as  $\varepsilon$ -caprolactam [50]. CPL-Cit and CPL-Lac show greater spectral alteration, especially in the O-H/N-H and C=O regions, indicating stronger molecular interactions and more complex hydrogen bonding networks [51,52], while CPL-For has a simpler spectrum, suggesting less interaction with caprolactam, possibly due to its lower number of functional groups [53]. CPL-Acet shows an intermediate behaviour, with interaction signals, but less intense than in CPL-Lac or CPL-Cit.

Fig. 4 shows the TGA curve of the  $\varepsilon$ -caprolactam-based ionic liquids. Thermogravimetric analysis (TGA) was used to evaluate the thermal stability of the four ILs evaluated in this work: CPL-Acet, CPL-Cit, CPL-For, CPL-Lac. Measurements were performed under an inert atmosphere, monitoring mass loss as a function of temperature. This allowed the determination of the degradation onset temperatures, primary thermal decomposition rates, and relative thermal stability of each system. The CPL-Lac system exhibited an initial mass loss of 4.20 % starting at 140.15 °C and remained thermally stable up to approximately 198.79 °C. The most significant mass loss occurred between 198.79 °C and 401.25 °C. The stabilization of the TGA curve beyond 400 °C suggests that no substantial additional mass loss occurred above this temperature. For the CPL-For system, a 7.80 % mass loss was observed at 136.50 °C, followed by rapid decomposition up to 270 °C. The reduced thermal stability is likely due to the high volatility and reactivity of formic acid, which can weaken its interactions with caprolactam. The CPL-Cit system showed an initial mass loss of 11.29 % up to 154.98 °C. The most substantial decomposition, accounting for 82.28 % of the total mass, occurred between 200  $^{\circ}$ C and 400  $^{\circ}$ C. The branched structure of citric acid promotes multiple interactions with caprolactam, enhancing the thermal resistance of the system [54,55]. In the case of CPL-Acet,

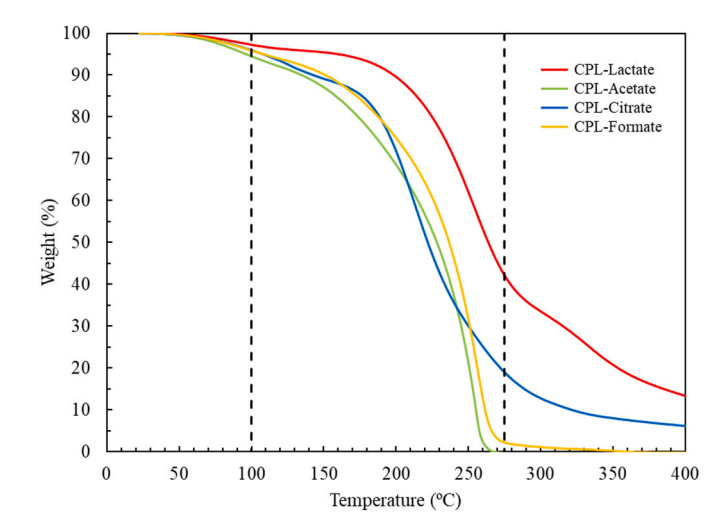


Fig. 4. TGA curves of the four  $\epsilon$ -caprolactam-based ionic liquids: Caprolactam (CPL)-Lactate; Caprolactam-Formate; Caprolactam-Citrate; Caprolactam-Acetate.

decomposition began around 150 °C, with the largest mass loss occurring between 180 °C and 300 °C. Although its stability exceeded that of CPL-For, it was inferior to that of CPL-Lac and CPL-Cit. This reduced stability can be attributed to the simpler structure of acetic acid, which limits its ability to form extensive hydrogen bonding networks with caprolactam. Previous studies, such as Zhang et al. [56] and Francisco et al. [57], have shown that organic acids with multiple functional groups, such as lactic and citric, when combined with hydrogen bond acceptors such as choline or lactams, lead to eutectic liquids with higher thermal stability. This supports the observation that the high stability of CPL-Lac can be attributed to the ability of lactic acid to establish strong and stable hydrogen bonding interactions with caprolactam.

Thermal analysis by differential scanning calorimetry (DSC) was employed to characterize the thermal behaviour and structural stability of ionic liquids (ILs) formed by caprolactam (CPL) and four carboxylic acids: acetic, citric, lactic, and formic acids. Six consecutive thermal cycles were performed (three heating and three cooling). The application of multiple thermal cycles in DSC is a common practice to evaluate the reversibility of thermal transitions and the stability of materials under repeated thermal stress. For ILs, this is particularly relevant due to their potential application in processes involving cyclic thermal changes. Repeated thermal cycles enable the detection of structural relaxation or molecular reorganization processes that may not be evident in a single cycle [58]. The first cycle allows for the identification of initial thermal transitions and behaviour during first melting, while cycles 2 and 3 assess thermal reversibility and IL stability, and cycles 4, 5, and 6 confirm the reproducibility of thermal events and reveal relaxations or the formation of new phases [59].

The DSC curve of CPL-Acetate (Fig. 5) in cycle 1 showed complex endothermic events, such as a sharp peak near 5 °C, attributed to partial melting of transient crystalline phases, and a broad depression around 55 °C, likely due to system reorganization. Additionally, an endothermic peak at  $-15.51~^{\circ}\text{C}$  with an inflection at  $-12.42~^{\circ}\text{C}$  indicated a glass transition. In cycle 3, an exothermic peak between -37.17 °C and 27.50 °C with  $\Delta H = 125.80$  mJ was detected, suggesting partial recrystallization. During cooling cycles 4 and 6, exothermic crystallization events were identified in the  $-30~^{\circ}\text{C}$  to  $-40~^{\circ}\text{C}$  range. These results suggest a strong capacity for structural organization upon cooling, forming a stable crystalline network suitable for applications requiring ordered structure and controlled thermal behaviour [60]. This behaviour implies favourable molecular symmetry and specific interactions between caprolactam and acetic acid that promote nucleation and crystalline growth [61]. Previous studies have shown that ILs with monocarboxylic acids tend to exhibit ordered structures due to reduced steric interference [62].

The results of the CPL-Citrate DSC curves (Fig. 5) showed a virtually invariant thermal behaviour, with no significant thermal transitions across all cycles. Cycle 1 displayed a slight endothermic event between  $-50\,^{\circ}\text{C}$  and  $-20\,^{\circ}\text{C}$  without a defined melting peak, and between  $44\,^{\circ}\text{C}$  and  $88\,^{\circ}\text{C}$ , a prominent endothermic event likely corresponding to the melting of a fraction that subsequently crystallized. This behaviour suggests that the mixture does not reach a defined molecular organization or forms an amorphous system, possibly due to the branched structure of citric acid with three carboxylic groups, which may hinder efficient molecular packing and formation of stable crystalline phases [63,64]. Such behaviour has been documented for ILs with polyfunctional or highly hydrogen-bonded structures [60].

On the other hand, the results of the curve of CPL-Lactate (Fig. 5) showed a well-defined thermal behaviour from the first cycle. A single endothermic peak was observed in cycle 1 within the  $-14~^{\circ}\text{C}$  to  $3~^{\circ}\text{C}$  range, consistent with a well-formed eutectic melting. The absence of additional transitions or changes in subsequent cycles indicates that the system reaches a thermodynamically stable configuration from the initial thermal stage, characteristic of well-defined and homogeneous ILs. This behaviour is desirable in materials requiring high thermal stability without phase transitions, such as amorphous solid electrolytes

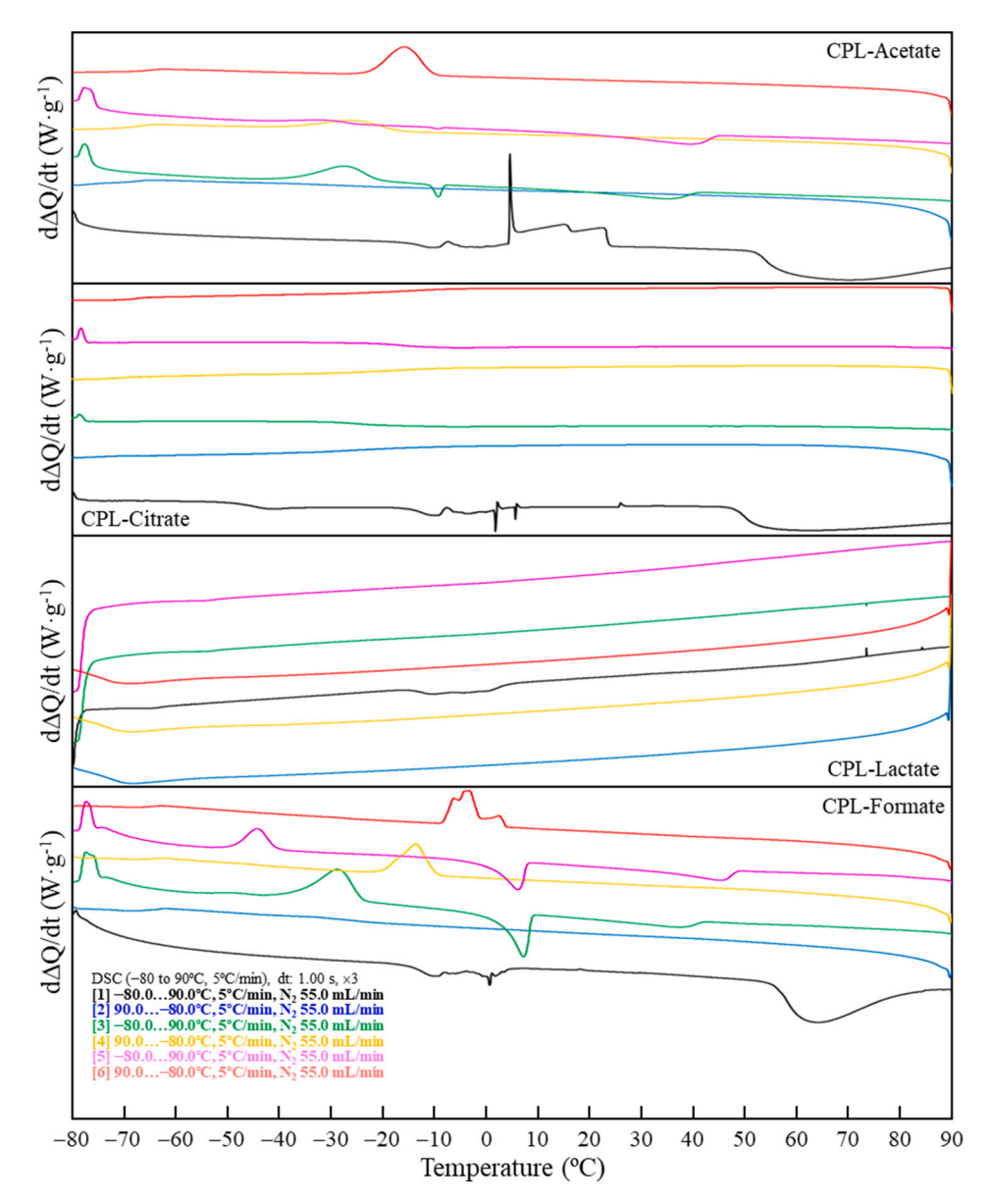


Fig. 5. DSC curve of the four ε-caprolactam-based ionic liquids: Caprolactam (CPL)-Lactate; Caprolactam-Formate; Caprolactam-Citrate; Caprolactam-Acetate.

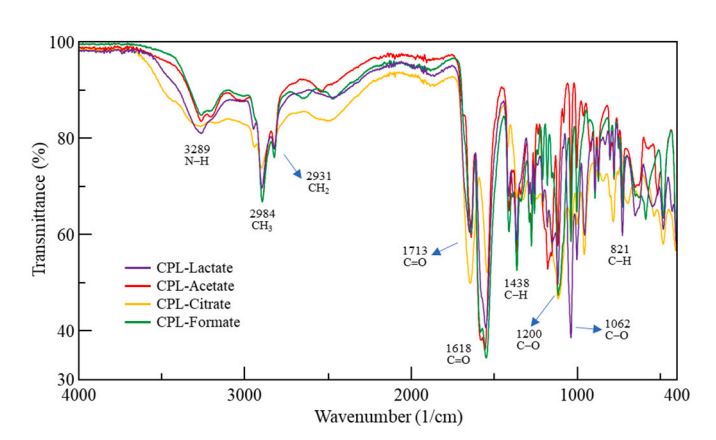


Fig. 6. FTIR spectra of the four  $\epsilon$ -caprolactam-based ionic liquids: Caprolactam (CPL)-Lactate; Caprolactam-Formate; Caprolactam-Citrate; Caprolactam-Acetate.

or uniform coatings. The relatively simple yet hydroxylated structure of lactic acid may facilitate the formation of disordered and crystallization-resistant hydrogen-bond networks [63,65].

The DSC curve of CPL-Formate (Fig. 5) showed a strong endothermic transition in cycle 1, with a melting peak centred at 63.50  $^{\circ}$ C, indicating the presence of a well-defined crystalline phase in the initial sample. In cycle 2, two exothermic events were identified, with main peaks at −18.00 °C and − 55.30 °C, corresponding to sequential crystallization processes, while cycle 3 revealed a less intense melting transition at 49.10  $^{\circ}\text{C},$  suggesting a less robust crystalline structure possibly due to incomplete crystallization in the previous cycle. In cycle 4, two crystallization events reappeared at -28.60 °C and - 70.40 °C, confirming the reproducibility of the phenomenon. Cycle 5 showed a weaker endothermic signal at 45.60 °C and a secondary transition at −40.80 °C, likely associated with molecular rearrangement before melting. Cycle 6 presented crystallization events with a main peak at -13.50 °C and a secondary signal at -48  $^{\circ}$ C, indicating higher energy release and a possibly more efficient reorganization of the solid phase. Overall, the CPL-Formate system exhibits high reversible crystallization capacity and well-defined melting behaviour, indicating a partially crystalline nature

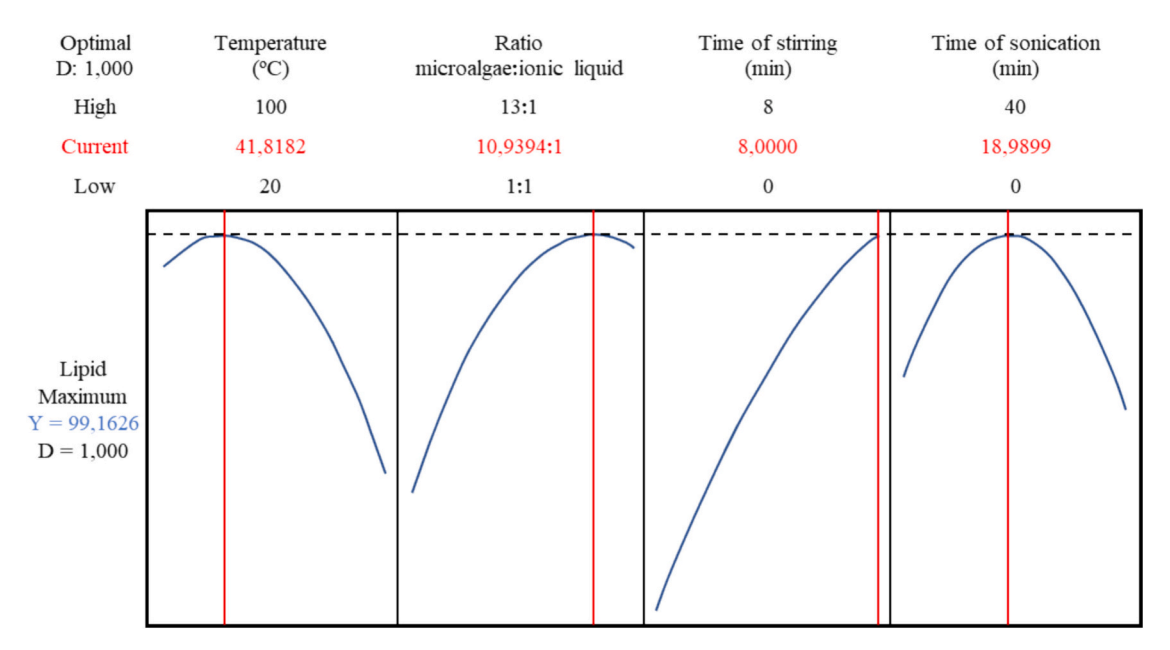


Fig. 7. Predicted process optimization of lipid extraction from starved Parachlorella kessleri using ε-caprolactam-lactate ionic liquid.

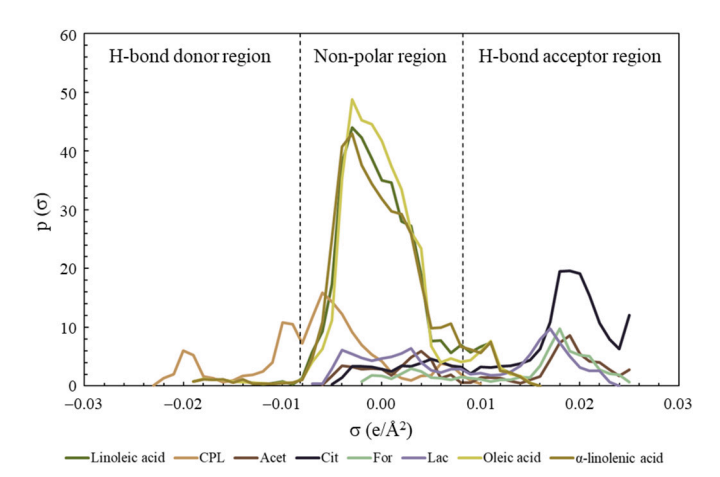


Fig. 8.  $\sigma$  profiles of the solutes oleic acid and linoleic acid, the cation  $\epsilon$ -caprolactam (CPL) and, the evaluated anions: acetate (Acet), citrate (Cit), formate (For) and, lactate (Lac).

with thermally reproducible features cycle after cycle [60].

The density of the CPL-Lac, CPL-For, CPL-Acet. And CPL-Cit ionic liquids were determined to be 1.25 g·cm $^{-3}$ ; 1.03 g·cm $^{-3}$ ; 1.01 g·cm $^{-3}$ ; 1.37 g·cm $^{-3}$  respectively at 20 °C using a calibrated pycnometer. The pH of the ionic liquids was measured as 3.00; 3.40; 4.51; 1.01 respectively using a potentiometric method with standard buffer calibration.

# 3.3. Screening of different $\varepsilon$ -caprolactam-based ionic liquids for the extraction of lipids from starved Parachlorella kessleri

## 3.3.1. Experimental screening

The four different caprolactam-based ILs were first evaluated in terms of lipid extraction ability from starved *Parachlorella kessleri*. The screening was conducted using microalgae that had been ultrasonicated for 15 min, mixing it with each IL at a 1:10 ratio for 4 h at 80  $^{\circ}$ C under constant magnetic stirring at 800 rpm.

Table 4 shows the results of the screening in the lipid extraction process in *Parachlorella kessleri*. The four caprolactam-based ILs presented very high lipid recovery results, all of them above 85 %. Among them, the highest recovery, 89.82 %, was achieved with CPL-Lac,

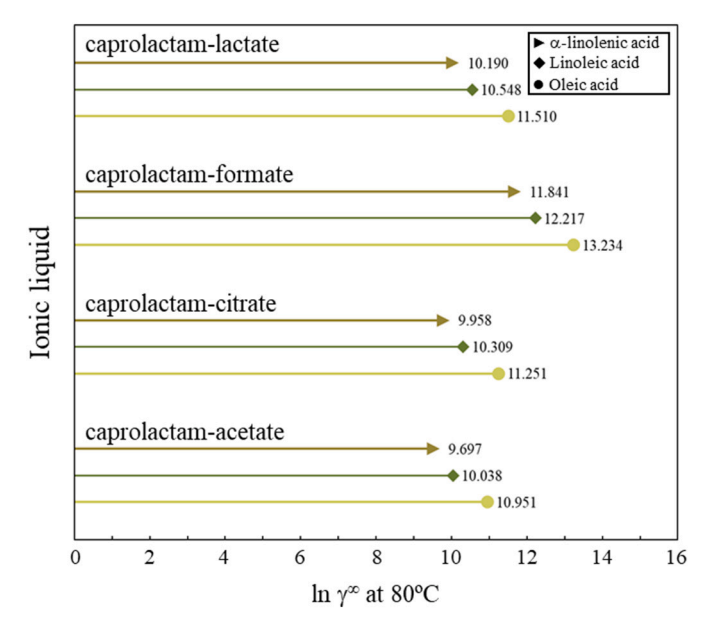


Fig. 9. Logarithmic infinite dilution activity coefficients (ln  $\gamma^{\infty}$ ) at 80 °C of  $\alpha$ -linolenic ( $\blacktriangleright$ ), linoleic ( $\spadesuit$ ) and oleic ( $\spadesuit$ ) acids in each of the evaluated caprolactam-based ionic liquids: caprolactam-lactate, caprolactam-formate, caprolactam-citrate and, caprolactam-acetate.

followed closely by the 88.61 %, 86.72 % and 85.86 % of CPL-Acet, CPL-Cit and CPL-For, respectively.

It must be noted, however, that the one-way analysis of variance (ANOVA) revealed that there were no statistically significant differences among the ILs used (F(3,80) = [1.39], p = 0.31), indicating that these ILs could be used indistinctively.

The results obtained in this study are consistent with previous studies on the use of  $\epsilon$ -caprolactam-based ILs for lipid extraction from microalgae. Naiyl et al. [29] worked on the extraction of lipids from Spirulina platensis using CPL-Acet, obtaining a lipid recovery of 14.20 % ( $w_{lipids}/w_{biomass}$ ), which was better than lipid extraction with just methanol and hexane, highlighting the potential that these ILs have for lipid extraction.

These slight differences in lipid extraction among the four ILs stem

Table 4
Screening of lipids extraction using different ε-caprolactam-based ionic liquids. Experimental conditions: Ratio: 1:10 g<sub>Microalgae</sub>/g<sub>Ionic Liquid</sub>; Temperature: 80 °C; Speed of stirring: 500 rpm; Time of stirring: 5 h; Time of sonication: 20 min.

Ionic liquid	Initial dry mass (g)	Weight of lipids (g)	Lipids recovered (%)**
Caprolactam-Lactate (CPL-Lac)	1.06	0.3340	$89.80\pm1.96$
Caprolactam-Formate (CPL-For)	1.07	0.3207	$85.90\pm3.5$
Caprolactam-Citrate (CPL-Cit)	1.06	0.3207	$86.70\pm4.07$
Caprolactam-Acetate (CPL-Ace)	1.03	0.3205	$88.60\pm2.29$

<sup>\*\*</sup>Calculated by: (% Lipids extracted \* 100)/ % lipids in the microalgae (34.83).

from the specific properties of each anion, as they vary in terms of hydrogen bonding ability, polarity and thermal stability, which are factors that can ultimately influence the lipid extraction performance.

Anions such as lactate, acetate, formate, and citrate vary in their hydrogen bonding ability, polarity, and thermal stability, factors that influence the lipid extraction efficiency from the microalgae starved *Parachlorella kessleri*. Such variables were evaluated in the COSMO-RS calculations of the upcoming section.

### 3.3.2. Theoretical ionic liquid screening with COSMO-RS calculations

COSMO-RS quantum chemical calculations were used as a tool to validate the experimental observations through the study of the  $\sigma$ -profiles of the cations, anions and solutes and the  $\ln\gamma^\infty$  of the solutes in each of the four ILs.

3.3.2.1.  $\sigma$  profiles of the cations, anions and solutes. Fig. 8 presents the  $\sigma$  profiles of the three solutes, the cation and the anions. Oleic, linoleic and  $\alpha$ -linolenic acid exhibit very similar  $\sigma$  profiles that align with those previously reported in the literature [66]. The three lipids present a large peak in the non-polar region ( $-0.0082\,\text{eÅ}^{-2} < \sigma < +0.0082\,\text{eÅ}^{-2}$ ) [67], although they also present some smaller peaks in the hydrogen bond acceptor region ( $+0.0082\,\text{eÅ}^{-2} < \sigma$ ). The difference in height among these peaks is due to the number of double bonds that these molecules have. Linoleic acid and  $\alpha$ -linolenic acid have two double bonds, which makes them more polar than oleic acid, which just has one [66].

As expected, caprolactam presented peaks in the hydrogen bond donor region, while the anions presented them in the hydrogen bond acceptor one. Following the principle that "like dissolve like" [68], the cation-anion combinations that would cover most of the  $\sigma$  profiles of the lipids would be the most suitable ones. In this regard, the huge peak of the citrate anion in the hydrogen bond acceptor area indicates that this IL would be a strong promotor of hydrogen bonding interactions with the lipids, as the peaks of the other ILs in this area are substantially narrower and smaller. In terms of non-polar interactions, the lactate anion presents the highest peaks, while the formate anion has the lowest.

Despite the broad peak of the citrate anion in the hydrogen bond acceptor area, CPL-Cit did not have a significantly higher experimental recovery than the other CPL-based ILs. This observation suggests that  $\sigma\text{-profiles}$  capture only part of the extraction mechanism, while extraction factors such as mass transport phenomena and the inherent complexity of working with biomass instead of model compounds contributed to levelling the experimental extraction performance across the different ILs. In this regard,  $\sigma\text{-profiles}$  should be considered qualitative indicators of potential solute-solvent interactions rather than as a complete mechanistic explanation of lipid recovery.

3.3.2.2. Prediction of the logarithmic infinite dilution activity coefficients ( $\ln \gamma^{\infty}$ ). The logarithmic form of the infinite dilution activity

coefficients (ln  $\gamma^{\infty}$ ) of the three major lipids in *Parachlorella kessleri*, oleic, linoleic and  $\alpha$ -linolenic acid, were predicted at 80 °C to study the impact of the IL anion on the extraction efficiency of lipids and compare the theoretical predictions with experimental performance. Lower ln  $\gamma^{\infty}$  indicate a higher affinity of the solute for the solvent, suggesting that COSMO-RS calculations could serve as a theoretical benchmark for interpreting extraction trends [69].

Fig. 9 presents the ln  $\gamma^{\infty}$  at 80 °C for the three major lipids. In all cases, the three lipids show the same affinity for each IL, with oleic acid having the highest values and  $\alpha$ -linolenic acid the lowest ones. Such observation could be linked to the polarity differences among these three lipids stemming from their number of double bonds, as discussed in the previous section.

According to the COSMO-RS calculations, the lipid affinity for the caprolactam-based ILs evaluated in this work follows the trend: CPL-Acet > CPL-Cit > CPL-Lac > CPL-For. This order is consistent with experimental results, with the only exception being CPL-Lac, which shifts from the highest experimental performance to the third position in the computational ranking. This observation highlights that, although corrected models like Lei2018 improve the accuracy of the predictions, they may still diverge from real system behaviour.

This switch in CPL-Lac classing can be attributed to two main factors: the closeness between the predicted  $\ln \gamma^{\infty}$  values, and the lack of statistically significant differences among experimental observations.

Considering both computational and the experimental results, CPL-Lac was selected for lipid extraction optimization due to its higher experimental performance.

# 3.4. Experimental design for the extraction of lipids from starved Parachlorella kessleri by caprolactam-lactate-based ionic liquid

An experimental design was done for the lipid extraction from starved *Parachlorella kessleri* using the best ionic liquid, previously tested and confirmed, ε-caprolactam lactic acid.

With the maximum and minimum values defined (see Section 2.4.3), the Minitab® program has provided 31 experiments with a single replicate, establishing a random order run. Based on the experimental design presented in Table SI1 (supplementary information), the experimental results of the lipid extractions at different conditions are also shown in Table SI1 (supplementary information).

The extraction of lipids from microalgae with ionic liquids has proven to be an efficient and environmentally friendly alternative to traditional methods using organic solvents. In this study, lipid extraction from starved *Parachlorella kessleri* has been optimized under different experimental conditions, using  $\varepsilon$ -caprolactam-lactate as ionic liquid. The best lipid recovery results (up to 94.4 %) were achieved with a combination of high temperature (80 °C), low biomass/IL ratio (1/10) and prolonged sonication (30 min).

These findings are consistent with previous studies in which ionic liquids have shown a significant impact on microalgae cell wall disruption, facilitating lipid release. Recent studies by Mohammadsaleh et al. [70], evaluated the use of ionic liquids in *Dunaliella salina*, where they showed efficiency in lipid extraction due to the ability to destabilize and permeabilize the cell wall of the microalgae, results that are consistent with those found in the extraction of lipids from starved *Paraclorella kessleri*. Compared to lipid extraction with conventional methods, it has been found in several studies that ionic liquids offer advantages such as high selectivity and lower environmental toxicity compared to other methods [71].

It can be observed that in the tests where the time of sonication is 30 min, a higher percentage of lipids was given with 31.65 % and 32.86 % in experiments 1 and 22, that sonication facilitates the rupture of cellular structures and allows greater contact of the ionic liquid with the lipids.

The temperature influenced the effect on the damage of the hydrogen bond network of cellulose and therefore influenced the efficiency of total

lipid extraction, this coincides with what was stated by Zhou et al. [72] who in their research found that there is a significant increase in lipid extraction during the first  $2\,h$ , when the temperature increased from 50 to 70 °C, improving the efficiency of lipid extraction from 13.50 to 17.00 % by using ionic liquids [BMIM][MeSO<sub>4</sub>].

Working with wet microalgae allows the water content to act as a polar solvent, decreasing the viscosity of the ionic liquid, thus enhancing its contact with the microalgae particles and therefore improving the lipid extraction efficiency. Furthermore, the presence of water allows the precipitation of cellulose and/or proteins, other valuable components, suggesting that the water contained in microalgae plays a key role in the extraction process using ionic liquids, in two different ways: as a solvent to decrease the viscosity of the ionic liquid and therefore improve the lipid efficiency; and as a polar solvent for the regeneration of other valuable components.

## 3.5. Process optimization

The Response Surface Methodology (RSM) was used to evaluate the effect of four process variables—temperature, biomass: ionic liquid ratio, stirring time, and sonication—on the percentage of lipid recovery from microalgae starved *Parachlorella kessleri*. The solvent used was an ionic liquid composed of  $\varepsilon$ -caprolactam and lactic acid, with the objective of identifying optimal conditions that maximize the efficiency of the extraction process.

The experimental results shown in Table SI1 (supplementary information) showed that stirring time had a significant effect on lipid recovery. For example, trial 4, with a stirring time of 6 h, achieved 96.20 % recovery, in contrast to trial 6 (2 h), which obtained only 72.30 %. Similarly, the biomass:ionic liquid ratio showed a marked influence, with intermediate values such as 1:10 and 1:7 being the most effective. In this regard, trials 4 and 22, with a 1:10 ratio, showed recoveries of 96.20 % and 94.40 %, respectively, far exceeding the values obtained with low ratios such as 1:1, where only 69.60 % was achieved.

Regarding the sonication variable, this was favourable, with most experiments that underwent 30-min sonication achieving lipid recovery percentages above 90 %. In contrast to experiment 1 (0-min sonication), where only 69.50 % was obtained. This suggests that cell disruption by ultrasound plays a key role in the efficiency of the process. Regarding the temperature variable, although temperatures up to  $100~^{\circ}\text{C}$  were explored, the optimal values ranged between  $40~^{\circ}\text{C}$  and  $80~^{\circ}\text{C}$ , as extreme temperatures, as in experiment 9 ( $100~^{\circ}\text{C}$ ), reduced the yield to 63.20 %, possibly due to thermal degradation of lipids.

Process optimization, based on experimental data obtained under different conditions, was carried out using Minitab® software. Table 5 and Fig. 7 present the optimal operating conditions determined by the model, the values presented in Table 5 correspond to the optimal conditions predicted by the response surface model in Minitab. They appear in duplicate due to the software's prediction procedure and do not represent independent experimental replicates. The study showed that the process using the ionic liquid of  $\epsilon$ -caprolactam and lactic acid in microalgae starved P. kessleri can achieve efficiencies comparable to or higher than those previously reported for other microalgal species. Furthermore, it is concluded that the application of sonication as a pretreatment, as well as the appropriate selection of temperature and biomass: ionic liquid ratio, are key factors for an efficient and scalable extraction process. These findings are consistent with those reported by

Valério et al. [73], who also applied RSM to optimize lipid extraction with ionic liquids, identifying contact time and sonication as the most influential parameters. According to the optimization performed in the present study, the optimal extraction parameters were 8 h of stirring and 19 min of sonication, a 1:11 ratio, and a temperature of 42 °C, which validates the reproducibility and industrial applicability of this methodology.

## 3.6. Esterification of the lipids extracted from starved Parachlorella kessleri

For biofuel production, only the saponifiable part of the total extracted lipids, fatty acid methyl esters (FAME), was considered, therefore, it is very important to determine the yields of saponifiable lipids and their composition. The results obtained from the transesterification reaction from the best experiments, and the optimal ones are shown in Table SI2 (supplementary information).

Generally, the recovery of FAMES was always higher than 60 %, except for experiments 16 and 19. In addition, it was affected by the conditions chosen. From experiment 31, the highest FAMES was obtained (78.10 %). From the optimum conditions, a similar value was obtained, around 77.70 %. Therefore, lower temperature and lower pretreatment (sonication) time imply longer agitation time in order to achieve the same results.

The identification and quantification of FAMEs obtained from *Parachlorella kessleri* by GC-FID are presented in Table 6 and Table SI3. The results show that the main fatty acid methyl esters present in the lipid extracts obtained through ionic liquids were palmitic acid (C16:0), stearic acid (C18:0), oleic acid (C18:1), linoleic acid in its trans (C18:2 trans) and cis (C18:2 cis) forms, as well as  $\alpha$ -linolenic acid (C18:3 n3), an omega-3 fatty acid with recognized biological relevance. Among all compounds, oleic acid methyl ester (C18:1) was the most abundant in most treatments, followed by linoleic derivatives. Similar results have been reported in other microalgae, where FAME profiles are dominated by C16:0, C18:1, and C18:0 [46].

When comparing the traditional Bligh & Dyer (B&D) method with ionic liquid-based extractions, remarkable differences can be observed. The B&D method showed a strong recovery of saturated fatty acids, particularly C16:0 and C18:0, which is consistent with previous reports indicating that classical solvent-based methods tend to favour the extraction of triglycerides and neutral lipids. While these compounds enhance the oxidative stability of biodiesel, they also increase the melting point and reduce cold flow properties, which may limit its application in low-temperature environments [74,75].

On the other hand, extractions using the  $\epsilon$ -caprolactam–lactic acid ionic liquid showed a more balanced profile between saturated and unsaturated fatty acids, with notable increases in C18:1cis + trans, C18:2trans, and C18:3n3. This behaviour is consistent with recent studies demonstrating that ionic liquids have an affinity for polar lipid fractions and glycolipids, which are rich in unsaturated fatty acids [76]. From the perspective of biodiesel quality, the presence of unsaturated fatty acids improves viscosity; however, a higher degree of unsaturation may compromise the oxidative stability of the fuel, increasing the risk of degradation during storage [77]. In contrast, the extraction with ionic liquids also yielded a good proportion of long-chain saturated FAMEs such as palmitic and stearic acids, which are highly desirable [72] because biodiesel with a high content of saturated fatty acids exhibits

Table 5
Lipid recovery results obtained from the optimal conditions of the experimental design of extraction of starved *Parachlorella kessleri* using  $\varepsilon$ -caprolactam-acid lactic ionic liquids.

Run N°	Experimental conditions	Results				
	Ratio biomass:ionic liquid	Temperature (°C)	Time of stirring (min)	Time of sonication (min)	Weight of lipids (g)	Lipids recovered (%)
Opt. 1	1:11	42	8	19	0.32	89.60
Opt. 2	1:11	42	8	19	0.33	91.80

D. Rivas-Navia et al.	Algal Research 92 (2025) 104369
-----------------------	---------------------------------

Table 6
GC-FID results of most important FAMES obtained from the best lipid extraction experiments from *Parachlorella kessleri*.

Experiment	FAME (%	6)											
	C14:0	C14:1	C16:0	C16:1	C17:1	C18:0	C18:1 cis + trans	C18:2 cis + trans	C18:3n3	C20:0	C20:1	C20:2	C24:1+ C22:6
B&D		0,46	20,06	0,45	1,12	8,43	21,83	26,21	11,54	0,38	0,31	0,40	0,33
1	1,00		16,76	0,49	2,05	4,80	27,25	24,85	20,98	0,27	0,17		
10	1,24		21,03	0,53	1,52	6,01	28,43	22,86	16,28	0,34	0,22		
11	1,03		14,60	0,53	0,32	2,02	4,42	27,16	25,73	21,79	0,26	0,18	0,23
15	1,04		18,04	0,50	1,86	5,19	27,56	24,34	19,27	0,30	0,19		0,19
16	1,26		21,33	0,52	1,53	6,07	27,95	22,51	16,29	0,34	0,22	0,07	
18	0,96		17,12	0,49	2,10	4,86	28,24	24,16	19,88	0,27	0,18		0,17
19			10,07	0,65	2,48	3,24	36,78	34,61	10,65				
22	0,97		16,51	0,50	2,23	4,68	27,83	24,59	20,95	0,26			
23			15,90	0,51	2,02	4,70	27,34	25,88	21,58	0,27	0,18		0,19
28			17,63	0,54	1,95	5,24	29,48	27,67	16,15				
31			18,90	0,55	1,44	5,91	32,22	22,64	14,87	0,35	0,27		1,16
OP1			18,14	0,55	2,50	5,10	25,71	27,81	18,18	0,27	0,17		
OP2			18,20	0,55	2,51	2,41	22,15	27,97	24,21	0,27	0,16		

greater oxidative resistance [78]. Therefore, achieving an appropriate balance between saturated and unsaturated fatty acids is crucial to ensure both the oxidative stability and the energy efficiency of the biofuel.

The optimal extraction conditions determined by the experimental design (OP1 and OP2) further confirmed the selectivity of the process toward the recovery of high-value FAMEs. OP1 showed a higher proportion of C18:1 (25.7 %), whereas OP2 was distinguished by a greater content of C18:3n3 (24.2 %) and C18:2trans (22.9 %), reflecting the capacity of the optimized process to adjust the balance between saturated and unsaturated fatty acids depending on the operating conditions.

#### 4. Conclusions

The design, synthesis, and characterization of  $\epsilon$ -caprolactam-based ILs was successful, and their stability was confirmed by  $^1H$  NMR,  $^{13}C$  NMR, FTIR, TGA and DSC, The ionic liquid  $\epsilon$ -caprolactam-lactate (CPL-Lac) stood out as the most efficient in extracting lipids from starved *Parachlorella kessleri*, with a recovery rate of 89.80 %.

The optimization process using response surface area (RSM) experimental design was based on 31 experimental conditions. The best result was obtained in round 4 at 40  $^{\circ}\text{C}$ , with a biomass:IL ratio of 1:10, 6 h of stirring, and 30 min of sonication. These conditions allowed achieving lipid recovery rates of 96.20 %.

Chromatographic analysis (GC-FID) of the FAMEs showed a predominance of palmitic (C16:0), stearic (C18:0), oleic (C18:1), linoleic (C18:2 trans), and  $\alpha\text{-linolenic}$  (C18:3 n3) acids. Computational results generated by COSMO-RS, together with experimental results, show that the  $\epsilon\text{-caprolactam-lactate}$  ionic liquid is a technologically viable, environmentally sustainable, and scalable alternative for biorefinery processes using microalgal biomass, within the framework of developing SAF production with high conversion efficiency and low environmental impact.

The results obtained in this research support the viability of ionic liquids as sustainable alternatives for lipid extraction in biofuel production.

## CRediT authorship contribution statement

Denisse Rivas-Navia: Writing – review & editing, Writing – original draft, Visualization, Validation, Methodology, Investigation, Formal analysis, Data curation, Conceptualization. Jacky CheikhWafa: Writing – review & editing, Writing – original draft, Visualization, Validation, Methodology, Investigation, Formal analysis, Data curation, Conceptualization. Alba Zurita: Writing – review & editing, Writing – original draft, Visualization, Validation, Methodology, Conceptualization.

**Esther Torrens:** Resources, Project administration, Methodology, Funding acquisition, Data curation. **Christophe Bengoa:** Writing – review & editing, Visualization, Validation, Supervision, Project administration, Methodology, Funding acquisition, Data curation, Conceptualization.

## **Declaration of competing interest**

The authors report no commercial or proprietary interest in any product or concept discussed in this article.

## Acknowledgements

The authors thank the AlgoSolis R&D facility (www.algosolis.com) which provided the *Parachlorella kessleri* biomass, and more particularly Jordan Prieto, Vladimir Heredia, Mariana Titica and Jeremy Pruvost for managing this part of the study. Denisse Rivas wishes to acknowledge University Rovira i Virgili for the Martí Franquès pre-doctoral scholarship (2021PMF-PIPF07). Alba Zurita thanks the European Union (NextGenerationEU program), the SEPE (Servicio Público de Empleo Estatal, Gobierno de España) and the URV for the pre-doctoral contract, 2022PMF-INV-09. Additionally, the authors are recognized by the Comissionat per a Universitats i Recerca del DIUE de la Generalitat de Catalunya (2021-SGR-200) and are financially supported by the Universitat Rovira i Virgili through the 2022PFR-URV-25 contract. Finally, this work has received funding from the European Union's Horizon Europe Research and Innovation Programme under Grant Agreement No. 101122101.

## Appendix A. Supplementary data

Supplementary data to this article can be found online at https://doi. org/10.1016/j.algal.2025.104369.

## Data availability

Data will be made available on request.

## References

- S. Becken, B. Mackey, What role for offsetting aviation greenhouse gas emissions in a deep-cut carbon world? J. Air Transp. Manag. 63 (2017) 71–83, https://doi.org/ 10.1016/j.jajrtraman.2017.05.009.
- [2] C. Yue, P. Sun, F. Li, Sulfonium ionic liquids, in: S. Zhang (Ed.), Encyclopedia of Ionic Liquids, Springer, Singapore, 2020, https://doi.org/10.1007/978-981-10-6739-6 125-1.
- [3] M. Wang, X. Ye, H. Bi, Z. Shen, Microalgae biofuels: illuminating the path to a sustainable future amidst challenges and opportunities, Biotechnol. Biofuels 17 (2024) 10, https://doi.org/10.1186/s13068-024-02461-0.

- [4] I. Abrantes, A.F. Ferreira, A. Silva, M. Costa, Sustainable aviation fuels and imminent technologies-CO<sub>2</sub> emissions evolution towards 2050, J. Clean. Prod. 313 (2021) 127937, https://doi.org/10.1016/j.jclepro.2021.127937.
- [5] J. Ahlström, Y. Jafri, E. Wetterlund, E. Furusjö, Sustainable aviation fuels—options for negative emissions and high carbon efficiency, Int. J. Greenh. Gas Control 125 (2023) 103886, https://doi.org/10.1016/j.ijggc.2023.103886.
- [6] S.D. Ríos, J. Castañeda, C. Torras, X. Farriol, J. Salvadó, Lipid extraction methods from microalgal biomass harvested by two different paths: screening studies toward biodiesel production, Bioresour. Technol. 133 (2013) 378–388, https://doi. org/10.1016/j.biortech.2013.01.093.
- [7] B. Chen, C. Wan, M.A. Mehmood, J.-S. Chang, F. Bai, X. Zhao, Manipulating environmental stresses and stress tolerance of microalgae for enhanced production of lipids and value-added products–a review, Bioresour. Technol. 244 (2017) 1198–1206, https://doi.org/10.1016/j.biortech.2017.05.170.
- [8] N. Marszalek, T. Lis, The future of sustainable aviation fuels, Combust. Engines 191 (2022) 29–40, https://doi.org/10.19206/CE-146696.
- [9] S.R. Motlagh, R. Khezri, M. Etesami, C. Yern Chee, S. Kheawhom, K. Nootong, R. Harun, Microwave-assisted extraction of lipid and eicosapentaenoic acid from the microalga *Nanochloropsis* sp. using imidazolium-based ionic liquids as an additive in water, J. Appl. Phycol. 36 (2024) 1709–1724, https://doi.org/10.1007/ \$10811-024-03244-8
- [10] M. Vitova, K. Bisova, S. Kawano, V. Zachleder, Accumulation of energy reserves in algae: from cell cycles to biotechnological applications, Biotechnol. Adv. 33 (2015) 1204–1218, https://doi.org/10.1016/j.biotechadv.2015.04.012.
- [11] S. Nagappan, S. Devendran, P.C. Tsai, H. Jayaraman, V. Alagarsamy, A. Pugazhendhi, V.K. Ponnusamy, Metabolomics integrated with transcriptomics and proteomics: evaluation of systems reaction to nitrogen deficiency stress in microalgae, Process Biochem. 91 (2020) 1–14, https://doi.org/10.1016/j. procbio.2019.11.027.
- [12] B.S. Sazzad, M.A. Fazal, A.S.M.A. Haseeb, H.H. Masjukia, Retardation of oxidation and material degradation in biodiesel: a review, RSC Adv. 6 (2016) 60244–60263, https://doi.org/10.1039/C6RA10016C.
- [13] X. Li, P. Přibyl, K. Bišová, S. Kawano, V. Cepák, V. Zachleder, M. Čížková, I. Brányiková, M. Vítová, The microalga Parachlorella kessleri – a novel highly efficient lipid producer, Biotechnol. Bioeng. 110 (2013) 97–107, https://doi.org/ 10.1002/bit.24595.
- [14] J. Folch, M. Lees, G.H. Sloane-Stanley, A simple method for the isolation and purification of total lipides from animal tissues, J. Biol. Chem. 226 (1957) 497–509, https://doi.org/10.1016/S0021-9258(18)64849-5.
- [15] E.G. Bligh, W.J. Dyer, A rapid method of total lipid extraction and purification, Can. J. Biochem. Physiol. 37 (1959) 911–917, https://doi.org/10.1139/o59-099.
- [16] A. Hara, N.S. Radin, Lipid extraction of tissues with a low-toxicity solvent, Anal. Biochem. 90 (1978) 420–426, https://doi.org/10.1016/0003-2697(78)90046-5.
- [17] G. Choudhary, J. Dhariwal, M. Saha, S. Trivedi, M.K. Banjare, R. Kanaoujiya, K. Behera, Ionic liquids: environmentally sustainable materials for energy conversion and storage applications, Environ. Sci. Pollut. Res. Int. 31 (2024) 10296–10316. https://doi.org/10.1007/S11356-023.
- [18] H. Tokuda, K. Hayamizu, K. Ishii, M.A.B.H. Susan, M. Watanabe, Physicochemical properties and structures of room temperature ionic liquids. 1. Variation of anionic species, J. Phys. Chem. B 108 (2004) 16593–16600, https://doi.org/10.1021/ ip047480r
- [19] T. Iimori, T. Iwahashi, K. Kanal, K. Seki, J. Sung, D. Kim, H.O. Hamaguchi, Y. Ouchi, Local structure at the air/liquid interface of room-temperature ionic liquids probed by infrared-visible sum frequency generation vibrational spectroscopy: L-alkyl-3-meth ylimidazolium tetrafluoroborates, J. Phys. Chem. B 111 (2007) 4860-4866
- [20] E. Kianfar, S. Mafi, Ionic liquids: properties, application, and synthesis, Fine Chem. Eng. 2 (2020) 21–29, https://doi.org/10.37256/fce.212021693.
- [21] X. Zeng, J. Li, N. Singh, Recycling of spent lithium-ion battery: a critical review, Crit. Rev. Environ. Sci. Technol. 44 (2014) 1129–1165, https://doi.org/10.1080/ 10643389.2013.763578.
- [22] X. Zheng, Z. Zhu, X. Lin, Y. Zhang, Y. He, H. Cao, Z.A. Sun, Mini-review on metal recycling from spent lithium-ion batteries, Engineering 4 (2018) 361–370, https://doi.org/10.1016/j.eng.2018.05.018.
- [23] H. Luo, H. Yin, R. Wang, W. Fan, G. Nan, Caprolactam-based Brønsted acidic ionic liquids for biodiesel production from jatropha oil, Catalysts 7 (2017) 102, https://doi.org/10.3390/catal7040102.
- [24] B. Liu, J. Zhao, F. Wei, Characterization of caprolactam based eutectic ionic liquids and their application in SO<sub>2</sub> absorption, J. Mol. Liq. 180 (2013) 19–25, https://doi. org/10.1016/j.molliq.2012.12.024.
- [25] P.K. Chotaray, S. Jella, R.L. Gardas, Physicochemical properties of low viscous lactam based ionic liquids, J. Chem. Thermodyn. 74 (2014) 255–262, https://doi. org/10.1016/j.jct.2014.02.009.
- [26] C. Zhang, M.J. Yu, X.Y. Pan, G. Wu, L. Jin, W. Gao, M. Du, J. Zhang, Regioselective mononitration of chlorobenzene using caprolactam-based Brønsted acidic ionic liquids, J. Mol. Catal. A Chem. 383 (2014) 101–105, https://doi.org/10.1016/j. molcata.2013.11.025.
- [27] M. Shankar, P.K. Chhotaray, A. Agrawal, R.L. Gardas, K. Tamilarasan, M. Rajesh, Protic ionic liquid-assisted cell disruption and lipid extraction from freshwater Chlorella and Chlorococcum microalgae, Algal Res. 25 (2017) 228–236, https://doi.org/10.1016/j.algal.2017.05.009.
- [28] Fl. Vieira, R. Guilherme, M. Neves, A. Rego, M. Abreu, J. Coutinho, S. Ventura, Recovery of carotenoids from brown seaweeds using aqueous solutions of surfaceactive ionic liquids and anionic surfactants, Sep. Purif. Technol. 196 (2018) 300–308, https://doi.org/10.1016/j.seppur.2017.05.006.

- [29] R. Naiyl, F. Kengara, K. Kiriamiti, Y. Ragab, Lipid extraction from microalgae using pure caprolactam-based ionic liquids and with organic co-solvent, PeerJ Anal. Chem. 4 (2021) e13, https://doi.org/10.7717/peerj-achem.13.
- [30] S. Rezaei Motlagh, R. Harun, D.R. Awang Biak, S.A. Hussain, W.A. Wan Ab Karim Ghani, R. Khezri, C. Devi Wilfred, A.A. Elgharbawy, Screening of suitable ionic liquids as green solvents for extraction of eicosapentaenoic acid (EPA) from microalgae biomass using COSMO-RS model, Molecules 24 (2019) 713, https:// doi.org/10.3390/molecules24040713.
- [31] S. Rezaei Motlagh, R. Harun, D.R. Awang Biak, S.A. Hussain, R. Omar, A. A. Elgharbawy, COSMO-RS based prediction for alpha-linolenic acid (ALA) extraction from microalgae biomass using room temperature ionic liquids (RTILs), Mar. Drugs 18 (2020) 108, https://doi.org/10.3390/md18020108.
- [32] S. Rezaei Motlagh, R. Harun, D.R. Awang Biak, S.A. Hussain, A.A. Elgharbawy, R. Khezri, C. Devi Wilfred, Prediction of potential ionic liquids (ILs) for the solid–liquid extraction of docosahexaenoic acid (DHA) from microalgae using COSMO-RS screening model, Biomolecules 10 (2020) 1149, https://doi.org/ 10.3390/biom10081149.
- [33] E.W. Rice, R.B. Baird, A.D. Eaton, L.S. Clesceri, Standard methods for the examination of water and wastewater, in: American Public Health Association, American Water Works Association, Water Environment Federation, W.C. Lipps, E. B. Braun-Howland, T.E. Baxter (Eds.), Standard Methods for the Examination of Water and Wastewater, 22nd ed., APHA Press, Washington DC, 2012.
- [34] M. DuBois, K.A. Gilles, J.K. Hamilton, P.A. Rebers, F. Smith, Colorimetric method for determination of sugars and related substances, Anal. Chem. 28 (1956) 350–356, https://doi.org/10.1021/ac60111a017.
- [35] O.H. Lowry, N.J. Rosebrough, A.L. Farr, R.J. Randall, Protein measurement with the Folin phenol reagent, J. Biol. Chem. 193 (1951) 265–275, https://doi.org/ 10.1016/S0021-9258(19)52451-6.
- [36] Z. Du, Z. Li, S. Guo, J. Zhang, L. Zhu, Y. Deng, Investigation of physicochemical properties of lactam-based Brønsted acidic ionic liquids, J. Phys. Chem. B 109 (2005) 19542–19546.
- [37] C.C. Pye, T. Ziegler, An implementation of the conductor-like screening model of solvation within the Amsterdam density functional package, Theor. Chem. Accounts 101 (1999) 396–408, https://doi.org/10.1007/s002140050457.
- [38] G.T. te Velde, F.M. Bickelhaupt, E.J. Baerends, C. Fonseca Guerra, S.J. van Gisbergen, J.G. Snijders, T. Ziegler, Chemistry with ADF, J. Comput. Chem. 22 (2001) 931–967, https://doi.org/10.1002/jcc.1056.
- [39] E.J. Baerends, N.F. Aguirre, N.D. Austin, J. Autschbach, F.M. Bickelhaupt, R. Bulo, C. Cappelli, A.C.T. van Duin, F. Egidi, C. Fonseca Guerra, A. Förster, M. Franchini, T.P.M. Goumans, T. Heine, M. Hellström, C.R. Jacob, L. Jensen, M. Krykunov, E. van Lenthe, A. Michalak, M.M. Mitoraj, J. Neugebauer, V.P. Nicu, P. Philipsen, H. Ramanantoanina, R. Rüger, G. Schreckenbach, M. Stener, M. Swart, J. M. Thijssen, T. Trnka, L. Visscher, A. Yakovlev, S. Gisbergen, The Amsterdam modeling suite, J. Chem. Phys. 162 (2025) (2025) 162501, https://doi.org/10.1063/5.0258496.
- [40] M. Diedenhofen, A. Klamt, COSMO-RS as a tool for property prediction of IL mixtures-a review, Fluid Phase Equilib. 294 (2010) 31–38, https://doi.org/ 10.1016/j.fluid.2010.02.002.
- [41] J. Han, C. Dai, G. Yu, Z. Lei, Parameterization of COSMO-RS model for ionic liquids, Green Energy Environ. 3 (2018) 247–265, https://doi.org/10.1016/j. gee.2018.01.001.
- [42] M. Olkiewicz, M. Caporgno, J. Font, J. Legrand, O. Lepine, N. Plechkova, J. Pruvost, K. Seddon, C. Bengoa, A novel recovery process for lipids from microalgæ for biodiesel production using a hydrated phosphonium ionic liquid, Green Chem. 17 (2015) 2813–2824, https://doi.org/10.1039/C4GC02448F.
- [43] W.W. Christie, X. Han, Lipid Analysis, in Isolation, Separation, Identification and Lipidomic Analysis, 4th ed., Oily Press Lipid Library Series, 2010.
- [44] C.H. Ra, C.H. Kang, J.H. Jung, G.T. Jeong, S.K. Kim, Effects of light-emitting diodes (LEDs) on the accumulation of lipid content using a two-phase culture process with three microalgae, Bioresour. Technol. 212 (2016) 254–261, https://doi.org/ 10.1016/j.biortech.2016.04.059.
- [45] J. Rawat, P.K. Gupta, S. Pandit, R. Prasad, V. Pande, Current perspectives on integrated approaches to enhance lipid accumulation in microalgae, 3 Biotech 11 (2021) 303, https://doi.org/10.1007/s13205-021-02851-3.
- [46] I.M.R. Fattah, M.Y. Noraini, M. Mofijur, A.S. Silitonga, I.A. Badruddin, T.M. Y. Khan, H.C. Ong, T.M.I. Mahlia, Lipid extraction maximization and enzymatic synthesis of biodiesel from microalgae, Appl. Sci. 10 (2020) 6103, https://doi.org/10.3390/app10176103.
- [47] D. Pal, I. Khozin-Goldberg, Z. Cohen, S. Boussiba, The effect of light, salinity, and nitrogen availability on lipid production by Nannochloropsis sp, Appl. Microbiol. Biotechnol. 90 (2011) 1429–1441, https://doi.org/10.1007/s00253-011-3170-1.
- [48] T. Takeshita, S. Ota, T. Yamazaki, A. Hirata, V. Zachleder, S. Kawano, Starch and lipid accumulation in eight strains of six *Chlorella* species under comparatively high light intensity and aeration culture conditions, Bioresour. Technol. 158 (2014) 127–134, https://doi.org/10.1016/j.biortech.2014.01.135.
- [49] A. Converti, A.A. Casazza, E.Y. Ortiz, P. Perego, M. Del Borghi, Effect of temperature and nitrogen concentration on the growth and lipid content of Nannochloropsis oculata and Chlorella vulgaris for biodiesel production, Chem. Eng. Process. Process Intensif. 48 (2009) 1146–1151.
- [50] L. Xu, J. Yin, Y. Luo, H. Liu, H. Li, L. Zhu, J. He, W. Jiang, W. Zhu, H. Li, Rational design of caprolactam-based deep eutectic solvents for extractive desulfurization of diesel fuel and mechanism study, ACS Sustain. Chem. Eng. 10 (2022) 4551–4560, https://doi.org/10.1021/acssuschemeng.1c08413.
- [51] B.N. Frandsen, A.M. Deal, J.R. Lane, V. Vaida, Lactic acid spectroscopy: intra- and intermolecular interactions, J. Phys. Chem. A 125 (2021) 218–229, https://doi. org/10.1021/acs.jpca.0c09341.

- [52] C. Tsioptsias, A. Panagiotou, P. Mitlianga, Thermal behavior and infrared absorbance bands of citric acid, Appl. Sci. 14 (2024) 8406, https://doi.org/ 10.3390/appl.4188406
- [53] A. Telfah, Q. Al Bataineh, K. Al-Essa, A. Al-Sawalmih, M. Telfah, M. Gogiashvili, A. Bahti, G. Majer, R. Hergenröder, <sup>1</sup>H and <sup>13</sup>C NMR and FTIR spectroscopic analysis of formic acid dissociation dynamics in water, J. Phys. Chem. B 128 (2024) 11417–11425, https://doi.org/10.1021/acs.jpcb.4c04701.
- [54] J.M. Halpern, R. Urbanski, A.K. Weinstock, D.F. Iwig, R.T. Mathers, H.A. Von Recum, A biodegradable thermoset polymer made by esterification of citric acid and glycerol, J. Biomed. Mater. Res. A 102 (2014) 1467–1477, https://doi.org/ 10.1002/jbm.a.34821.
- [55] R. Ortega-Toro, S. Collazo-Bigliardi, P. Talens, A. Chiralt, Influence of citric acid on the properties and stability of starch-polycaprolactone based films, J. Appl. Polym. Sci. 133 (2016) 42220, https://doi.org/10.1002/app.42220.
- [56] M. Zhang, X. Zhao, S. Tang, K. Wu, B. Wang, Y. Liu, Y. Zhu, H. Lu, B. Liang, Structure–properties relationships of deep eutectic solvents formed between choline chloride and carboxylic acids: experimental and computational study, J. Mol. Struct. 1273 (2023) 134283, https://doi.org/10.1016/j.
- [57] M. Francisco, A. van den Bruinhorst, M.C. Kroon, Low-transition-temperature mixtures (LTTMs): a new generation of designer solvents, Angew. Chem. Int. Ed. 52 (2013) 3074–3085, https://doi.org/10.1002/anie.201207548.
- [58] K. Machanová, Z. Wagner, A. Andresová, J. Rotrekl, A. Boisset, J. Jacquemin, M. Bendová, Thermal properties of alkyl-triethylammonium bis {(trifluoromethyl) sulfonyl} imide ionic liquids, J. Solut. Chem. 44 (2015) 790–810, https://doi.org/ 10.1007/s10953-015-0323-3
- [59] M. Clough, K. Geyer, P. Hunt, J. Mertes, T. Welton, Thermal decomposition of carboxylate ionic liquids: trends and mechanisms, Phys. Chem. Chem. Phys. 15 (2013) 20480–20495, https://doi.org/10.1039/C3CP53648C.
- [60] C. Yuanyuan, M. Tiancheng, Comprehensive investigation on the thermal stability of 66 ionic liquids by thermogravimetric analysis, Ind. Eng. Chem. Res. 53 (2014) 8651–8664, https://doi.org/10.1021/ie500959.
- [61] T. Greaves, C. Drummond, Protic ionic liquids: properties and applications, Chem. Rev. 108 (2008) 206–237, https://doi.org/10.1021/cr068040u.
- [62] T. Greaves, C. Drummond, Protic ionic liquids: evolving structure-property, Chem. Rev. 115 (2015) 11379–11448, https://doi.org/10.1021/acs.chemrev.5b00158.
- [63] A. Andresová, M. Bendová, J. Schwarz, Z. Wagner, J. Feder-Kubis, Influence of the alkyl side chain length on the thermophysical properties of chiral ionic liquids with a (1R, 2S, 5R)-(-)-menthol substituent and data analysis by means of mathematical diagnostics, J. Mol. Liq., 242 (2917) 336–348. doi:https://doi.org/10.1016/j. mollia.2017.07.012.
- [64] C. Xu, Z. Cheng, Thermal stability of ionic liquids: current status and prospects for future development, Processes 9 (2021) 337, https://doi.org/10.3390/pr9020337.
- [65] G.G. Eshetu, S. Jeong, P. Pandard, A. Lecocq, G. Marlair, S. Passerini, Comprehensive insights into the thermal stability, biodegradability, and combustion chemistry of pyrrolidinium-based ionic liquids, ChemSusChem 10 (2017) 3146–3159.

- [66] H. Xing, X. Zhang, Q. Yang, R. Liu, Z. Bao, B. Su, Y. Yang, Q. Ren, Separation of long chain fatty acids with different number of unsaturated bonds by fractional extraction: experimental and COSMO-RS study, Food Chem. 143 (2014) 411–417, https://doi.org/10.1016/j.foodchem.2013.08.009.
- [67] X. Liu, Y. Nie, Y. Liu, S. Zhang, A.L. Skov, Screening of ionic liquids for keratin dissolution by means of COSMO-RS and experimental verification, ACS Sustain. Chem. Eng. 6 (2018) 17314–17322, https://doi.org/10.1021/ acsuschemeng 8b04830
- [68] V. Rapinel, N. Rombaut, N. Rakotomanomana, A. Vallageas, G. Cravotto, F. Chemat, An original approach for lipophilic natural products extraction: use of liquefied n-butane as alternative solvent to n-hexane, LWT-Food Sci. Technol. 85 (2017) 524–533, https://doi.org/10.1016/j.lwt.2016.10.003.
- [69] D. Rodríguez-Llorente, A. Bengoa, G. Pascual-Muñoz, P. Navarro, V.I. Águeda, J. Delgado, A. Álvarez-Torrellas, J. García, M. Larriba, Sustainable recovery of volatile fatty acids from aqueous solutions using terpenoids and eutectic solvents, ACS Sustain. Chem. Eng. 7 (2019) 16786–16794, https://doi.org/10.1021/ acssuschemeng.9b04290.
- [70] F. Mohammadsaleh, A. Shadi, L. Nazari, Lipid extraction from Dunaliella salina using ionic liquids and deep eutectic solvents, J. Appl. Phycol. 37 (2025) 899–912, https://doi.org/10.1007/s10811-025-03477-1.
- [71] V. Ponnumsamy, H. Al-Hazmi, S. Shobana, J. Dharmaraja, D. Jadhav, R. Banu, G. Piechota, B. Igliński, V. Kumar, A. Bhatnagar, K. Chae, G. Kumar, A review on homogeneous and heterogeneous catalytic microalgal lipid extraction and transesterification for biofuel production, Chinese J. Catal. 59 (2024) 97–117, https://doi.org/10.1016/S1872-2067(23)64626-1.
- [72] W. Zhou, Z. Wang, A. Alam, J. Xu, S. Zhu, Z. Yuan, S. Huo, Y. Guo, L. Qin, L. Ma, Repeated utilization of ionic liquid to extract lipid from algal biomass, Int. J. Polym. Sci. 2019 (2019) 9209210, https://doi.org/10.1155/2019/9209210.
- [73] A. Valério, I. Vieitez, Â.P. Matos, J.V. Oliveira, Lipids and fatty acids from microalgae, in: J.A.V. Costa, B.G. Mitchell, J. Benemann (Eds.), Microalgal Bioengineering, Springer, Cham, 2024, https://doi.org/10.1007/978-3-031-61253-4 11.
- [74] G.F. Ferreira, L.F. Ríos Pinto, R. Maciel Filho, L.V. Fregolente, A review on lipid production from microalgae: association between cultivation using waste streams and fatty acid profiles, Renew. Sust. Energ. Rev. 109 (2019) 448–466, https://doi. org/10.1016/j.rser.2019.04.052.
- [75] L. Leng, W. Li, H. Li, S. Jiang, W. Zhao, Cold flow properties of biodiesel and the improvement methods: a review, Energy Fuel 34 (2020) 10364–10383, https:// doi.org/10.1021/acs.energyfuels.0c01912.
- [76] M.H.M. Eppink, S.P.M. Ventura, J.A.P. Coutinho, R.H. Wijffels, Multiproduct microalgae biorefineries mediated by ionic liquids, Trends Biotechnol. 39 (2021) 1131–1143, https://doi.org/10.1016/j.tibtech.2021.02.009.
- [77] K. Gaurav, K. Neeti, R. Singh, Microalgae-based biodiesel production and its challenges and future opportunities: a review, Green Technol. Sustain. 2 (2024) 100060, https://doi.org/10.1016/j.grets.2023.100060.
- [78] Mostafa S., N. El-Gendy, Evaluation of fuel properties for microalgae Spirulina platensis bio-diesel and its blends with Egyptian petro-diesel, Arab. J. Chem. 10 (2017) S2040–S2050, https://doi.org/10.1016/j.arabjc.2013.07.034.